STRESS VARIATION ALONG THE LENGTH

OF MODEL PILES

By

LAITH ISMAIL NAMIQ

Bachelor of Science

University of Baghdad

Baghdad, Iraq

1959

Submitted to the faculty of the Graduate School of
the Oklahoma State University
in partial fulfillment of the requirements
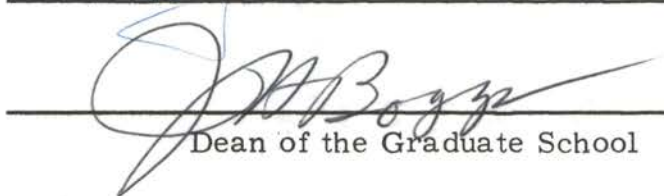for the degree of
MASTER OF SCIENCE
May, 1965

STRESS VARIATION ALONG THE LENGTH

OF MODEL PILES

Thesis Approved:

James V. Parcher
Thesis Adviser

R. L. Janes

J. M. Bogzz
Dean of the Graduate School

ACKNOWLEDGMENT

The writer wishes to express his sincere gratitude and deep appreciation to his advisor, Professor J. V. Parcher, a gentleman and a scholar. Only by his guidance, encouragement, loan of reference material, and interest in this research was the writer able to accomplish what he has.

The writer also wishes to thank,

The Government of Iraq for the scholarship which made his higher education possible.

The Oklahoma State University Development Foundation for providing financial support for the research.

Professor G. G. Smith for his valuable instruction in the use of strain gauges.

Professor R. L. Janes for his valuable instruction in graduate study and for the loan of reference material.

Mr. R. W. Thompson for his valuable help during the first stage of the investigation.

His family for their encouragement and understanding.

Mrs. Peggy Harrison for her accurate typing of the manuscript.

TABLE OF CONTENTS

iv

LIST OF TABLES

LIST OF PLATES

LIST OF FIGURES

CHAPTER I

INTRODUCTION

General

The problem of determining the load capacity of driven piles has received a great deal of attention in the technical literature. This problem has been discussed in a large number of articles, and several so-called dynamic and static formulas have been proposed and used (1). However, the mere existence of such varied and diverse formulas indicates that the complexity of the problem is so great that no single formula is likely to be adequate for all situations and all kinds of piles.

The basic variables governing the loading capacity of driven piles were correctly appraised by a number of investigators. In general, the ultimate load capacity of a pile is a function of the toe bearing, the skin friction, and the shear strength along the circumferential area of the displaced soil shell. The degree of importance of the various factors noted above depends on the type of soil, the geometry of the pile, the method of driving, the nature of loading, and the lapse of time between driving and loading. The primary factor for the ultimate bearing capacity is the toe bearing when the piles are supported on a very firm stratum, e.g., rock. These piles are mainly end bearing piles. The primary factor for the ultimate bearing capacity is skin friction when the piles are driven so that their

1

toes are not supported by a very firm stratum. These piles fall under the category of friction piles. For piles driven in a soil where the adhesion between the soil and the pile is of a greater magnitude than the shear strength of the soil itself, the primary factor for the ultimate bearing capacity is the shear strength along the circumferential area of the displaced soil shell. However, these factors may act jointly, each contributing to some extent to the ultimate bearing capacity of the driven pile.

<div align="center">Load Tests on Full Scale Piles</div>

In order to study the behavior of piles under working conditions, load tests on instrumented piles have been conducted. Crandall (2) reported the applicability of the use of strain gauges to measure the load transferred from concrete friction piles to the surrounding soil. Van Weele (3), utilizing electric extensometers on concrete piles, reported the confirmation of a method of separating the bearing capacity of a pile into ultimate point resistance and skin friction. Seed and Reese (4) used SR-4 strain gauges on several six inch diameter pipes, 20 feet long, used as displacement type friction piles driven into non-sensitive clay. They reported that the supporting capacity determined by multiplying the area of the embedded pile by the soil shear strength, obtained from unconfined compression tests of undisturbed samples, must be considered as an approximation, although it is nearly equal to the true supporting capacity in some instances. They also reported that for small values of time for shallow depths, the failure of the friction pile when overloaded did

not occur in the soil but at the interface between the pile and the soil. Vey (5) utilized SR-4 strain gauges on a steel H-pile driven through medium clay to end bearing in very hard soil. He reported that the load capacity determined from the shear strength of the soil applied to the effective section of the pile (formed by a line connecting the outside edges of the flanges) gives good agreement with observed data. Mansur and Kaufman(6) utilized strain rods on H sections, steel pipe, and precast concrete piles driven to a sand layer through layers of sandy silts, silty sands, and clay. They reported that considerable load was carried by skin friction at the silt layer and that the skin friction decreased near the pile tip in sand. Mohane, Jain, and Kumar (7) investigated cast in-situ concrete piles. The distribution of skin friction and point resistance for various loads was investigated by the use of wire resistance gauges, and they reported that the bearing capacity of the pile was attained by skin friction and point bearing. D'Appolonia and Romuldi (8) utilized SR-4 strain gauges in end bearing steel H-piles driven 40 feet through sand and gravel. They reported that as much as one-third of the applied load did not reach the pile tip, and that the computed transferred load, using a maximum shear strength limitation for the soil, is in good agreement with test results. D'Appolonia and Haribar (9) utilized strain gauges to measure the load transferred from a step taper pile to the adjacent soil of an upper layer of dense sand and gravel and a lower layer of weathered shale, and reported that the load transferred along the length of this end bearing pile was appreciable.

Load Tests on Model Piles

Load tests on model piles have also been carried out. Mueller (10) used 80 cm (32 inches) long metal piles which were constructed in such a manner that the load could be applied separately, but not simultaneously, to the pile point or to the pile shell, or to the entire pile as a whole. The results reported were the average frictional resistance and the point bearing of the pile.

Khalifa (11) used sectional timber piles to determine the distribution of frictional forces along the length of a model pile. Bellows type pressure cells connected the pile sections. The piles were not driven, but sand was packed around them. The friction force per unit area between the pile and the sand was reported to be constant for the entire embedded length under a given load, to be independent of depth and to vary directly with the load. Davis and Webster (12) performed tests with a model pile which was similar to the one used by Mueller (10) except that one proving ring measured the total load applied and was operated simultaneously with a second proving ring which measured the fraction of the load carried by the pile point. The pile was not driven, but jacked into dry sand to the required depth. Krome (13) employed a composite steel pile 30 inches long and 1.5 inches in diameter. The load fractions carried by the pile shell and the pile point were measured by two pairs of thin metal strips with SR-4 strain gauges attached to them. The total force of friction was measured and the pile settlement was recorded. The test was mainly to investigate the potentialities of the SR-4 strain gauges and the possibility of their use on model piles. Florentin, L'Heriteau, and Farhi (14) employed brass tube elements of 42 mm diameter (external) and 97 mm length. These elements were

welded without fins or couplings. Each element bore two diametrically

opposite SR-4 strain gauges, with an SR-4 strain gauge at the tip of

the pile. The piles were driven in sand and the frictional resistance

under consecutive cycles of loading and unloading was recorded. They

found that the lateral frictional resistance and the point resistance

appeared at the same time. The lateral friction distribution was not

parabolic as predicted by theory at the ultimate bearing capacity of

the pile. They also reported that for two piles of different lengths,

but with the same total imposed load, the lateral frictional resistance

curves do not superpose. The ratio of the lateral resistance to the

point resistance of the shorter pile was less than that of the longer

pile, and the point resistance of the shorter pile greater than that of

the longer pile.

Ghanem (15) used one-fourth inch diameter steel rods embedded

11 inches in clay. He compared the observed skin friction on the

embedded area of the pile with the shear strength of the clay. The

failure load was calculated by the ultimate load method on the basis

of the vane shear test. The shear strength, S, determined by

$S = \frac{F}{\pi\,d\,H}$; where F = ultimate bearing, d = diameter, H = depth of

embedment, and S = shear strength; for the single pile was, on the

average 18% more than the shear strength as determined by the vane.

El Din (16) used polished oak models 0.5 inch in diameter, and 10

inches long, driven in fat clay, and reported that the ultimate bearing

capacity of these friction piles equalled the resistance due to the

adhesion between the soil and the pile shaft in addition to the load

sustained by the toe of the pile and the shearing resistance along the

circumferential area of a displaced clay shell having a volume equal to that of the penetrating pile. This later force represents more than 80% of the ultimate bearing capacity of a friction pile.

Nature and Scope of the Investigation

The general behavior, stresses, and strains along the length of model piles instrumented with SR-4 strain gauges and driven in cohesive and noncohesive soils are investigated. The tests were designed to provide further information regarding the stress variation along the piles in an attempt to gain additional knowledge to aid in the design of pile foundations.

CHAPTER II

MATERIALS AND EXPERIMENTAL PROGRAM

Clay

The clay used was Permian Red Clay, obtained from the basement of the Life Science Building on the Oklahoma State University campus at Stillwater, Oklahoma. The clay was dried to a constant moisture content of 2.83%. It was then pulverized and passed through a No. 30 sieve. Figure 1 shows a hydrometer analysis of the soil. Some of the properties of the clay are listed in Table I (17).

Sand

The sand used was rounded grain, uniform white quartz sand. It was used without any modification. Figure 2 shows the grain size distribution of the sand.

Model Piles

Three model piles were fabricated from a steel tube of 0.5 inch outside diameter and one-thirty-second inch wall thickness. The tube was cut into sections 18.0 inches long, and was then split lengthwise into two halves to facilitate the mounting of the strain gauges. Solid steel cones 0.433 inches long with a vertex angle of 60° degrees were manufactured and fitted at one end of each model pile as a tip. Steel caps 2.0 inches long and 0.75 inches outside diameter capped

7

TABLE I

Properties of Clay

Liquid Limit	40.5
Plastic Limit	15.0
Plasticity Index	25.5
Maximum γ_{dry} lbs/cu.ft.*	110.0
M.C.$_{optimum}$ %*	17.0
Specific Gravity	2.72
Percent < 0.002 mm	30

* Standard Proctor Compaction Test
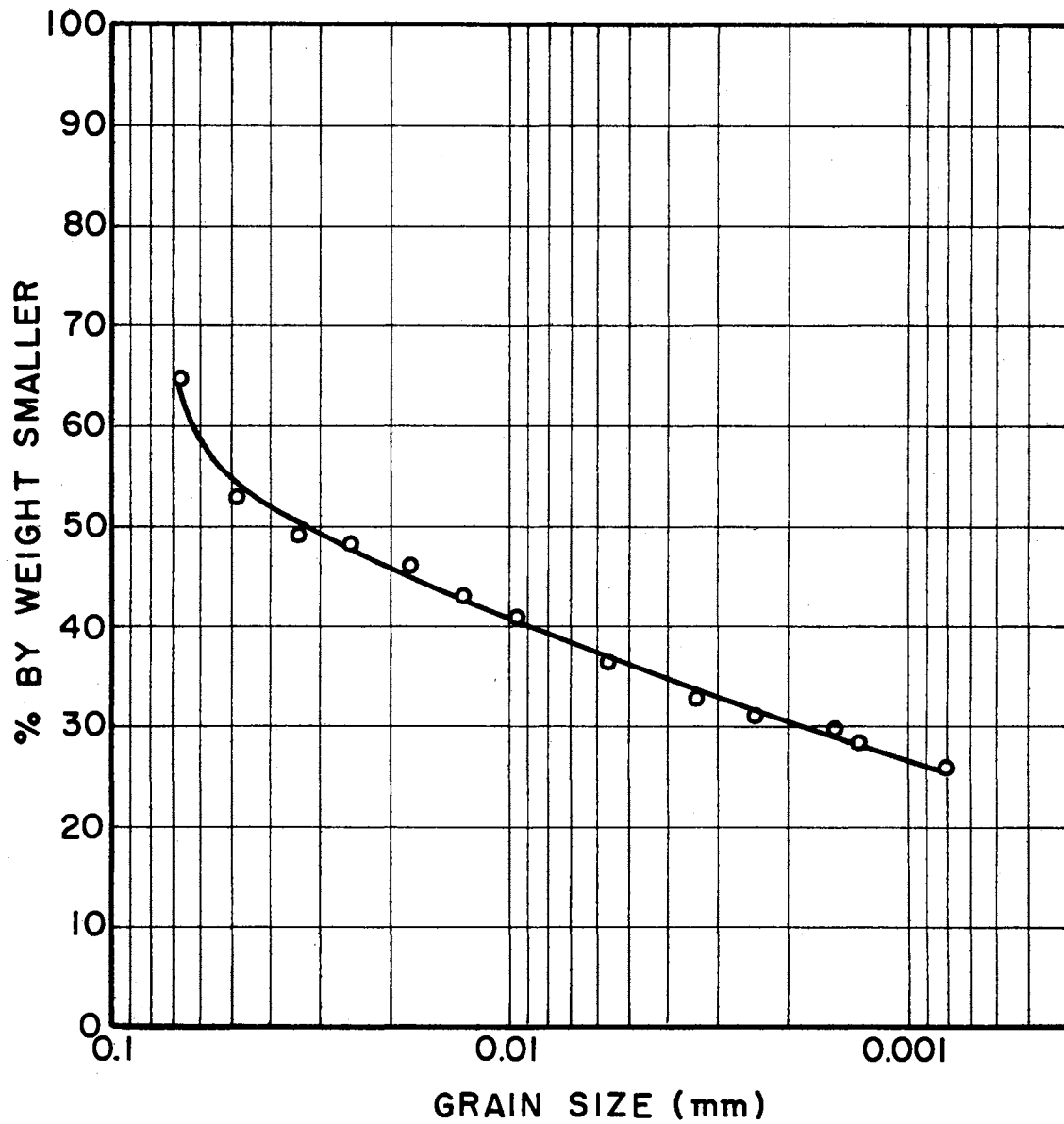
FIGURE I

GRAIN SIZE DISTRIBUTION CURVE FOR
PERMIAN RED CLAY
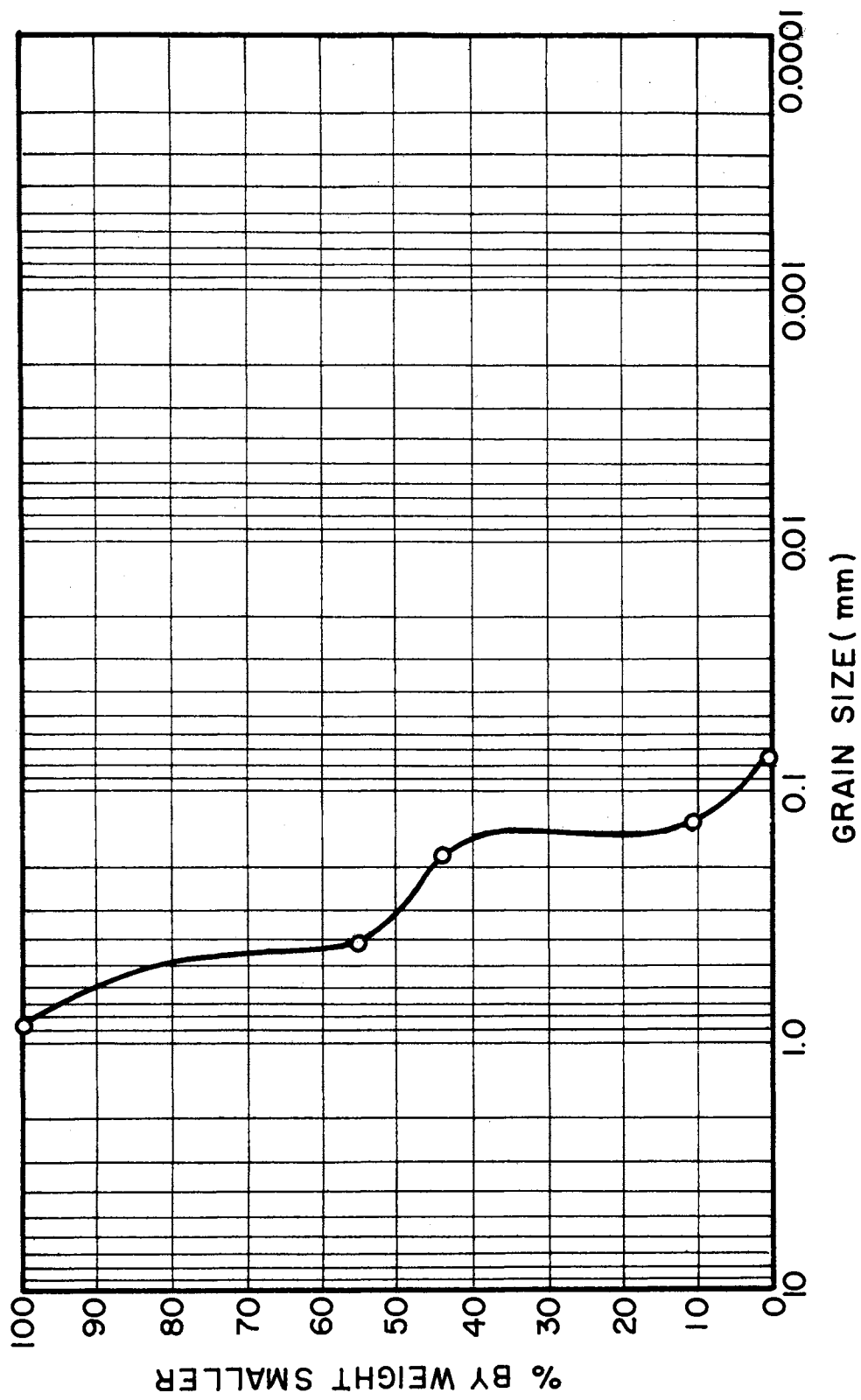
FIGURE 2

GRAIN SIZE DISTRIBUTION CURVE FOR SAND

the top end of each pile.

Loading Device

An aluminum beam having a cross section of one by two inches was utilized as a loading device. One end of the beam was supported at the wall by means of a 0.75 inch diameter hinge pin in a needle bearing which allowed the bar to rotate freely in a vertical plane. A hanging rod with a loading platform was similarly connected to the other end of the beam. The load was applied to the pile through a ball joint connected to a bracket which in turn was connected to the beam. Since the ball joint was located at one-third the distance between the hinge pins at either end, the ratio of the load applied at the loading platform to the load applied at the pile cap was 1:3. Plate (1) shows the loading device.

Instrumentation of the Model Piles

For the measurement of load at various points along the pile, type C6-111, temperature compensated, one-thirty-second of an inch SR-4 strain gauges were employed in the experimentation. Ten strain gauges were mounted in pairs having diametrically opposed members along the internal surface of each pile. The paired gauges were mounted at distances of 1.5, 6.0, 10.5, 15.0, and 17.0 inches from the tip. The gauges at the extremities were kept some distance away from the two ends of the pile as a precaution against possible effects of stress concentration, and possible damage by impact. Epoxy cement was utilized to put the two halves of each pile together,

PLATE 1
LOADING DEVICE
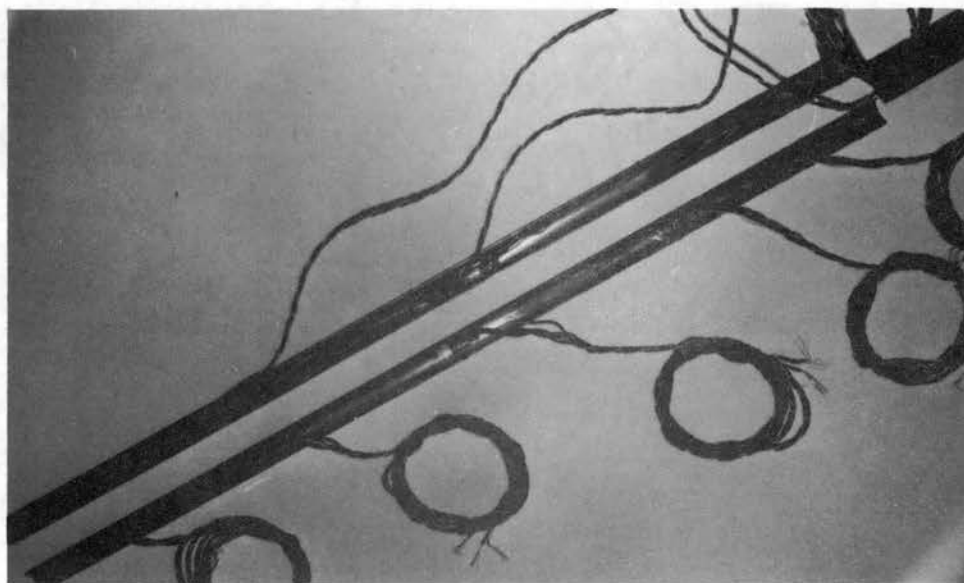
PLATE 2
EXPLODED VIEW OF MODEL PILE

and to secure the tip and cap to the pile. The wires leading from the strain gauges to the reading instrument were passed through an opening on the side of the pile cap. The final total length of each pile was 20.18 inches. Plate (II) shows the various parts of the model pile.

Calibration of Strain Gauges

The strain gauges were calibrated by dead weight as each pile was loaded as a column by increments of an axial load applied at the cap. A separate calibration curve, based on the average reading, was prepared for each pair of strain gauges. Figures 3 through 16 show the calibration curves for each pair of strain gauges.

Preparation of Soil Samples

Clay

The clay was compacted into a cylindrical container 13.5 inches in diameter, in 4.0 inch layers using a 10.0 lb. drop hammer having a free fall of 18.0 inches. Each layer received 50 blows. The clay sample was built up to a height of 20 inches. The unit weight of the soil sample was 100.0 lbs/cu.ft. with a moisture content of 17.0%.

The shear strength of the soil as obtained from quick undrained triaxial tests conducted on undisturbed samples taken from the container was 2.2 tons/sq.ft.

Sand

Dry sand was compacted in a container 14.0 inches in diameter
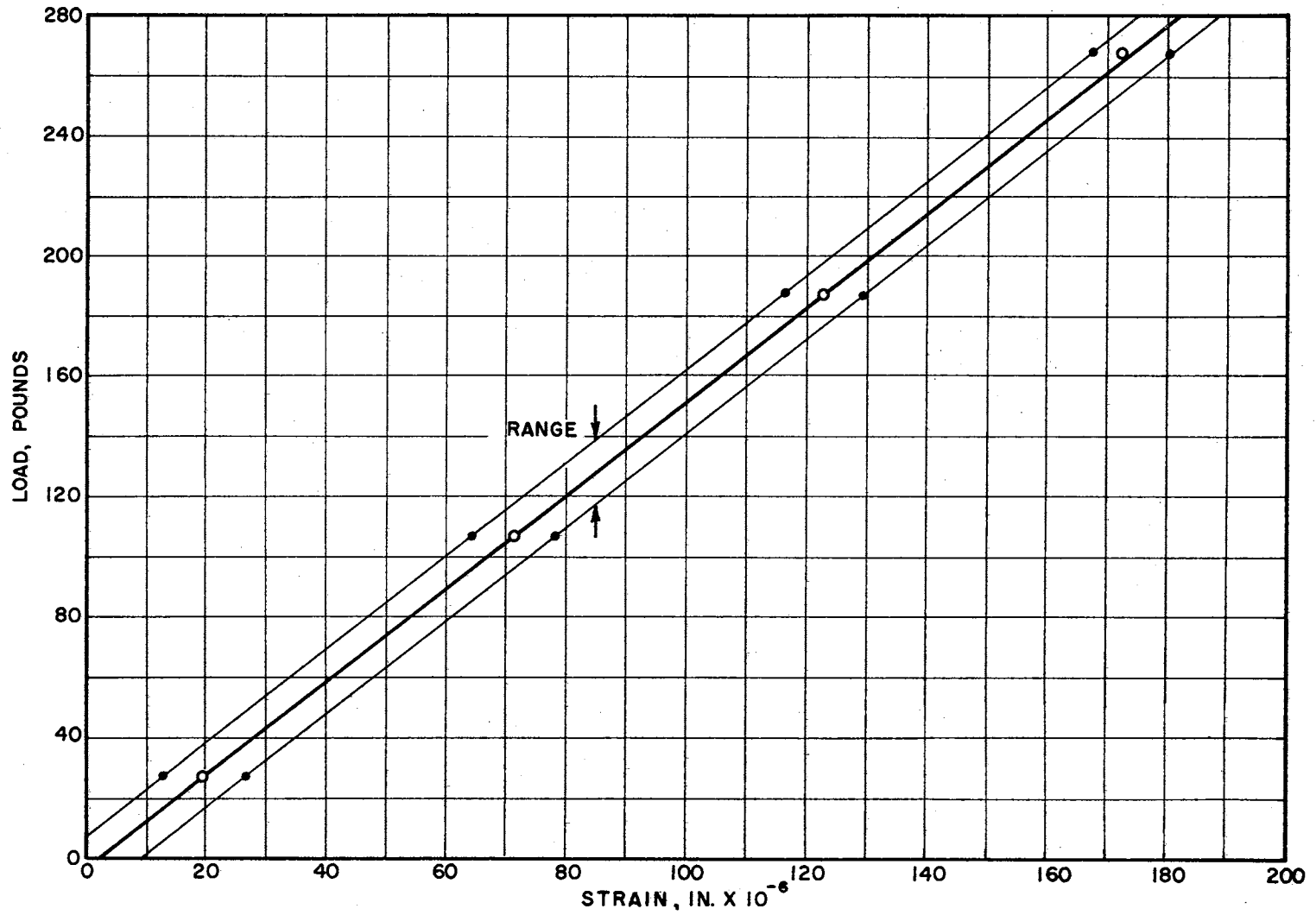
FIGURE 3
CALIBRATION CURVE FOR GAUGE 1S1 AND 1S2.(PILE NO. 1)
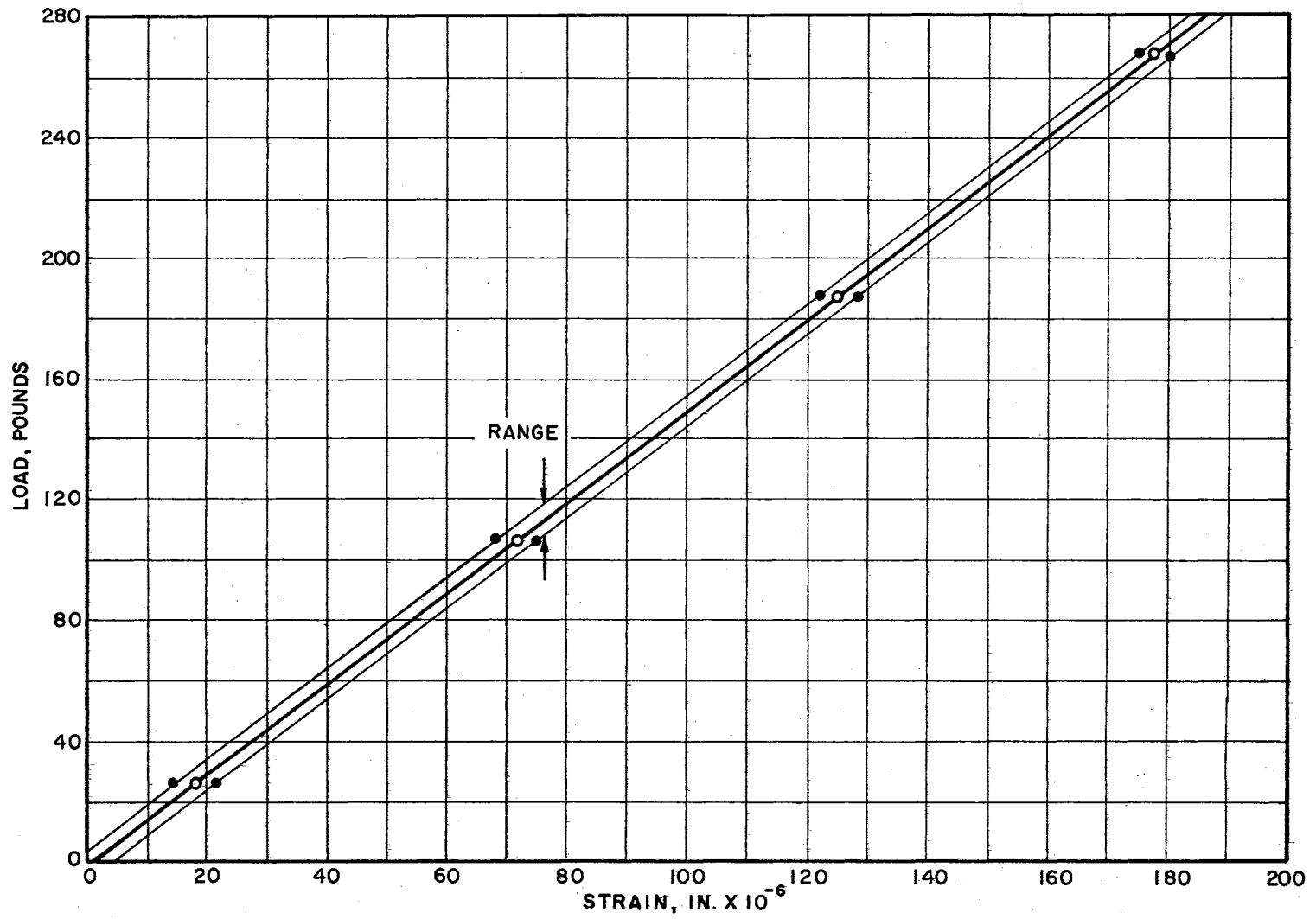
FIGURE 4

CALIBRATION CURVE FOR GAUGE 2S1 AND 2S2.(PILE NO.1)
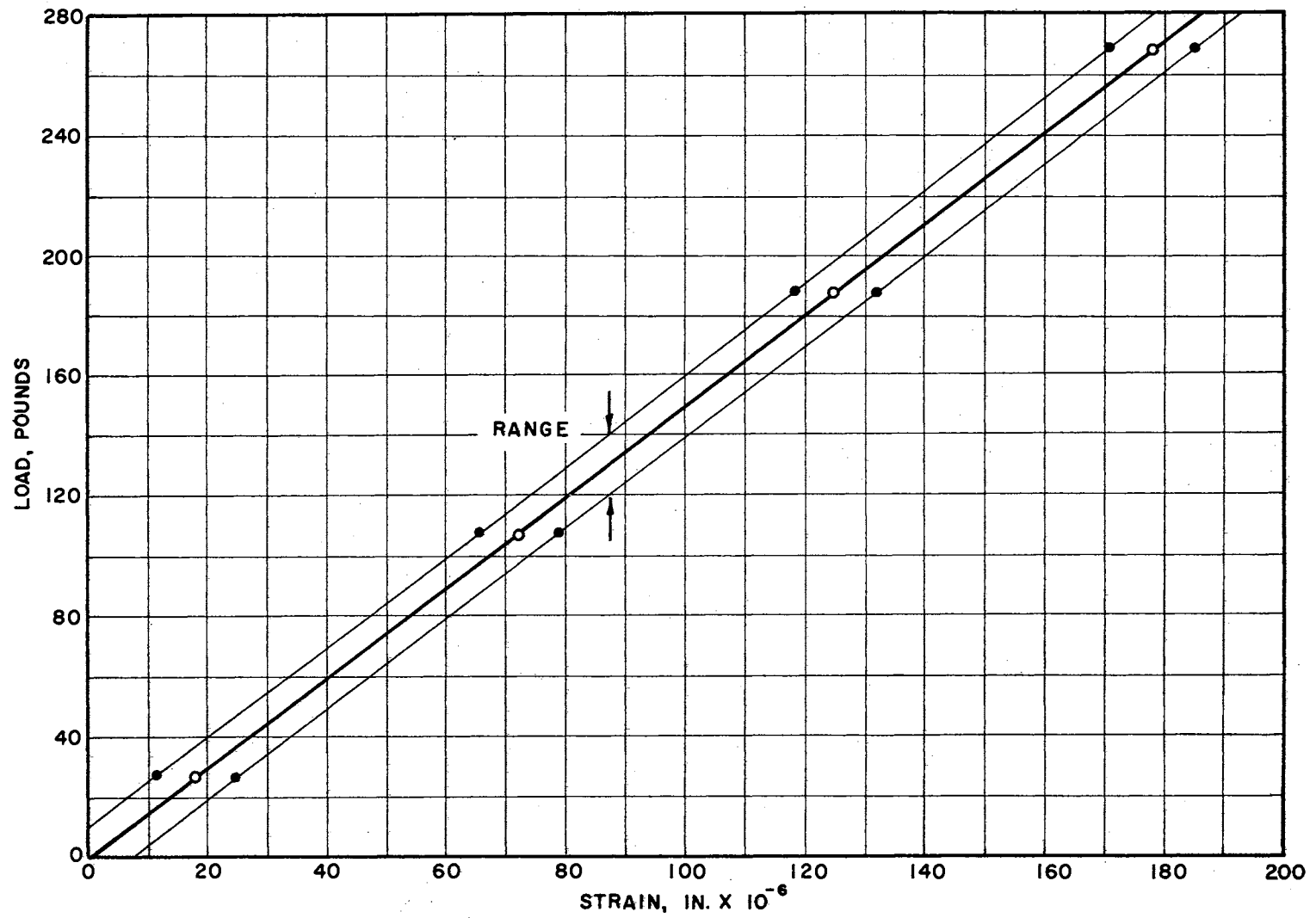
FIGURE 5

CALIBRATION CURVE FOR GAUGE 3S1 AND 3S2. (PILE NO.1)

16
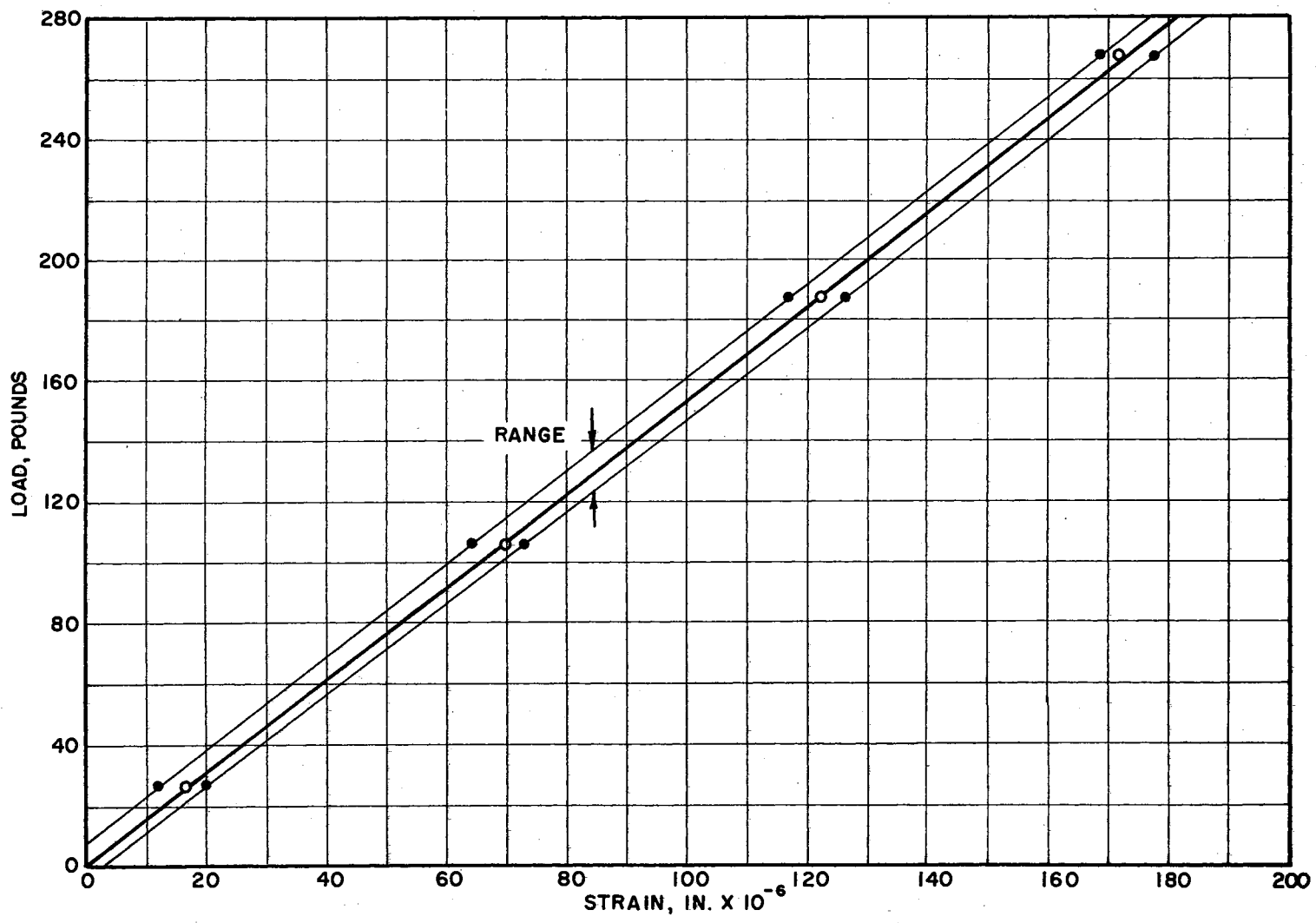
FIGURE 6

CALIBRATION CURVE FOR GAUGE 4S1 AND 4S2. (PILE NO.1)
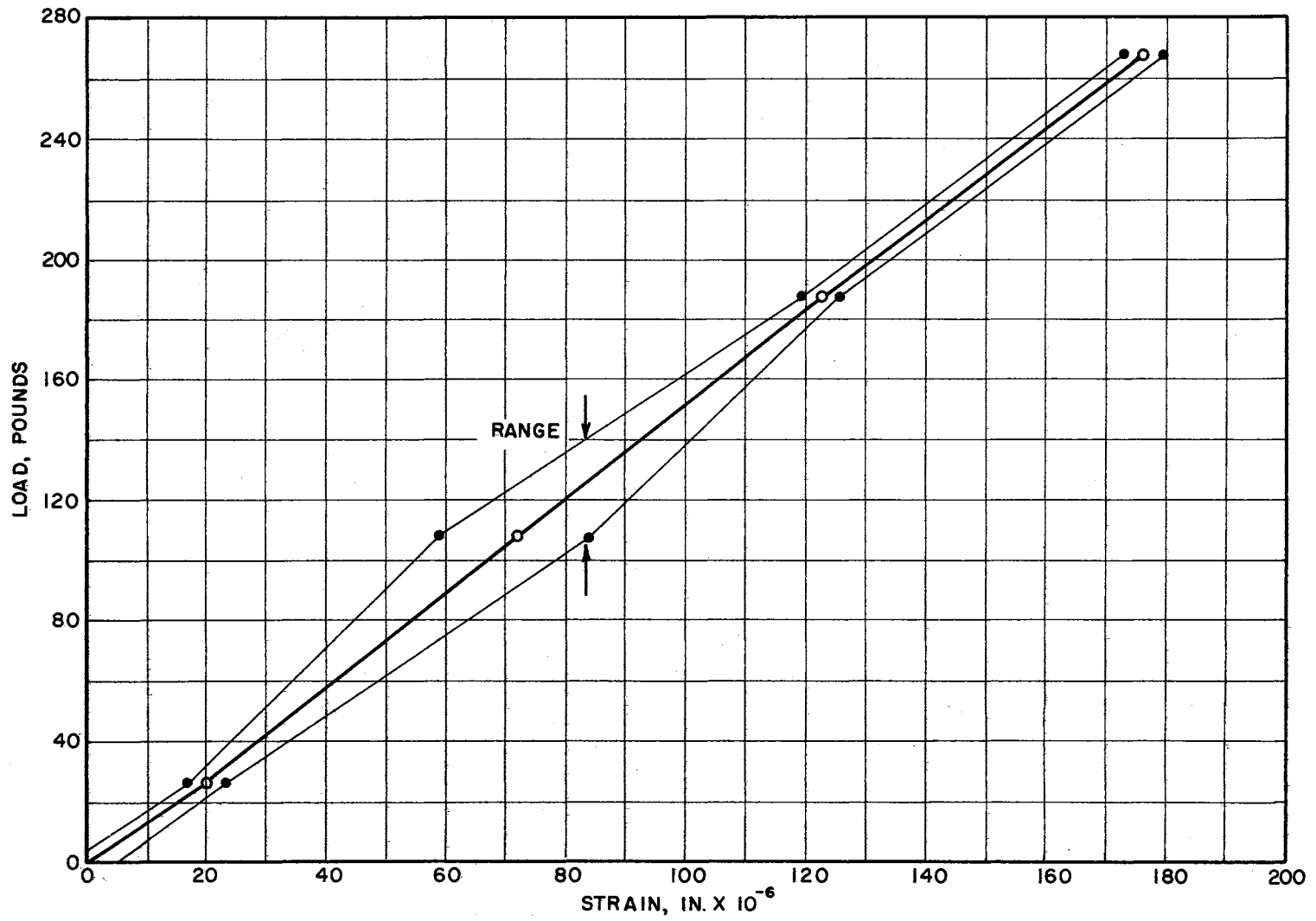
FIGURE 7

CALIBRATION CURVE FOR GAUGE 5S1 AND 5S2. (PILE NO. 1)
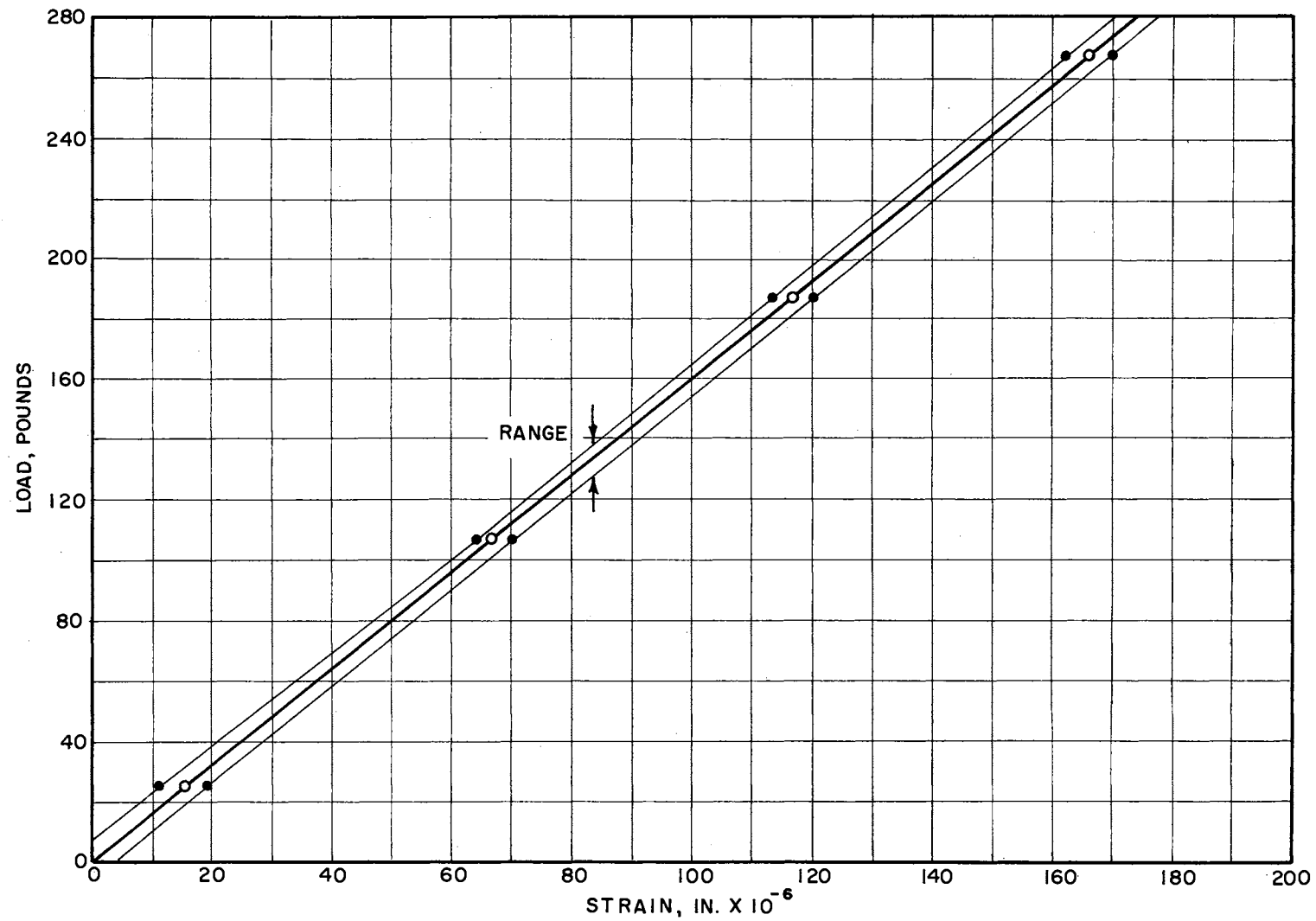
FIGURE 8

CALIBRATION CURVE FOR GAUGE 1S1 AND 1S2.(PILE NO. 2)

FIGURE 9

CALIBRATION CURVE FOR GAUGE 2S1 AND 2S2.(PILE NO.2)
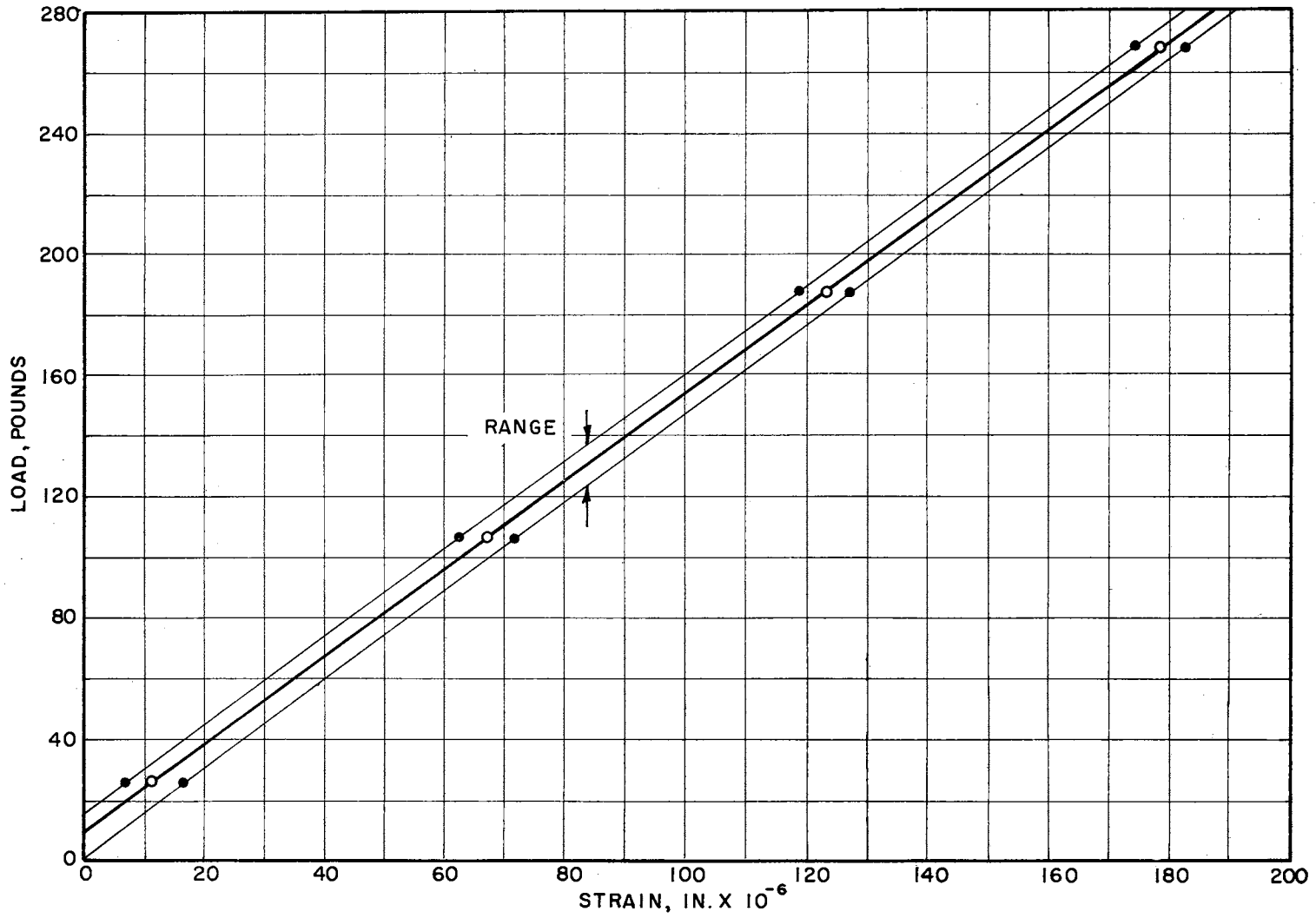
FIGURE 10

CALIBRATION CURVE FOR GAUGE 3S1 AND 3S2. (PILE NO. 2)
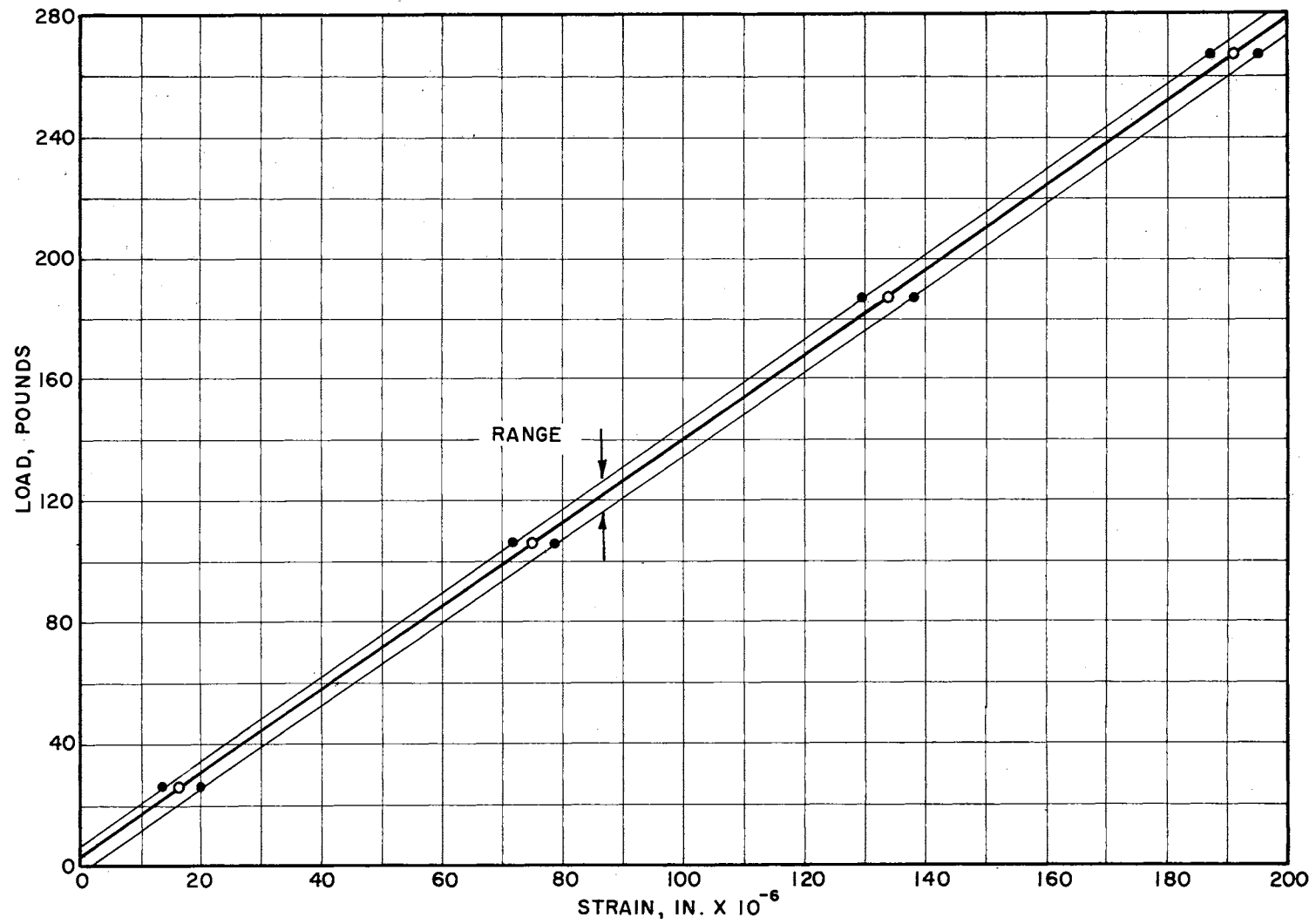
FIGURE II
CALIBRATION CURVE FOR GAUGE 4S1 AND 4S2. (PILE NO. 2)
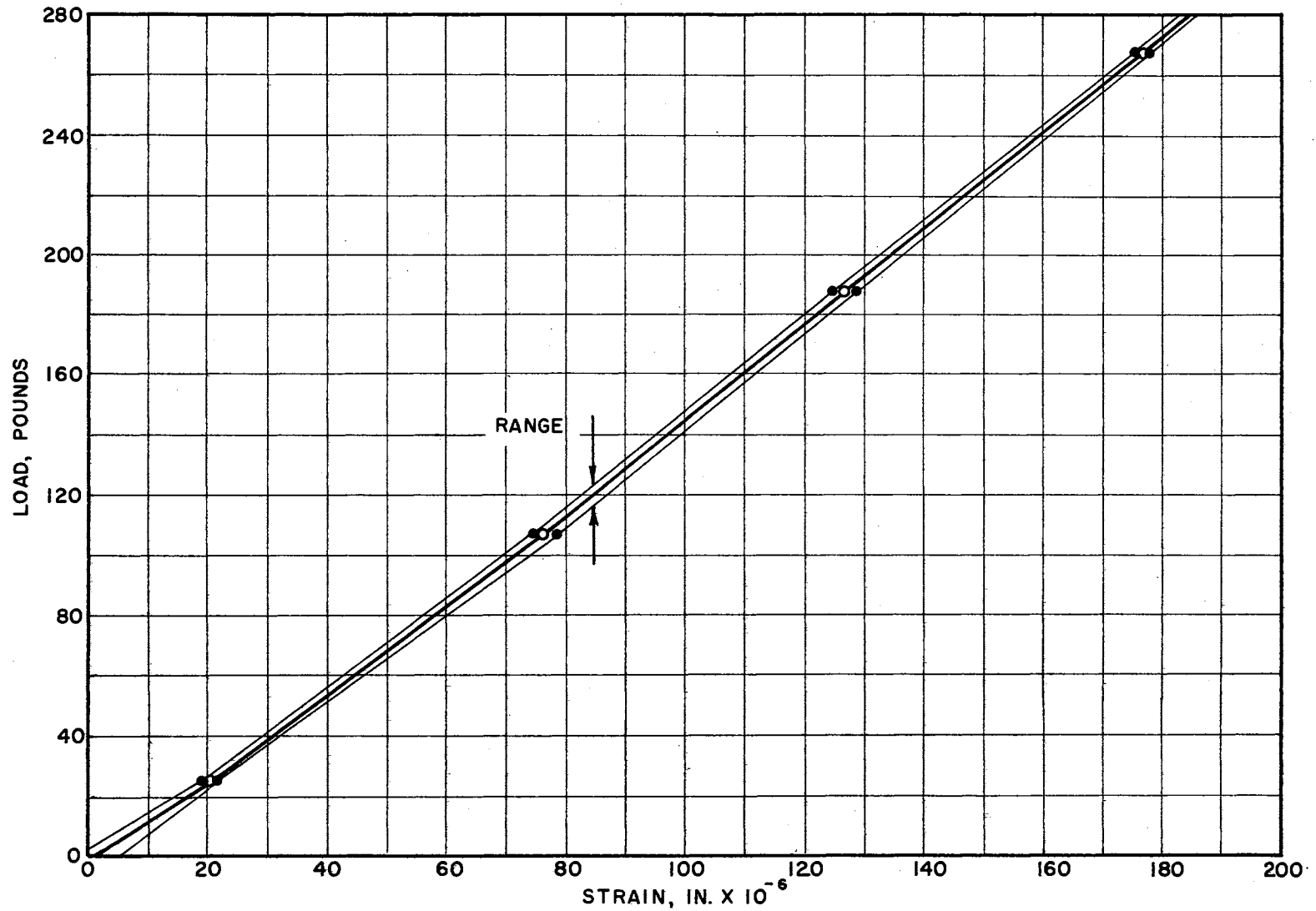
FIGURE 12

CALIBRATION CURVE FOR GAUGE ISI AND IS2. (PILE NO. 3)
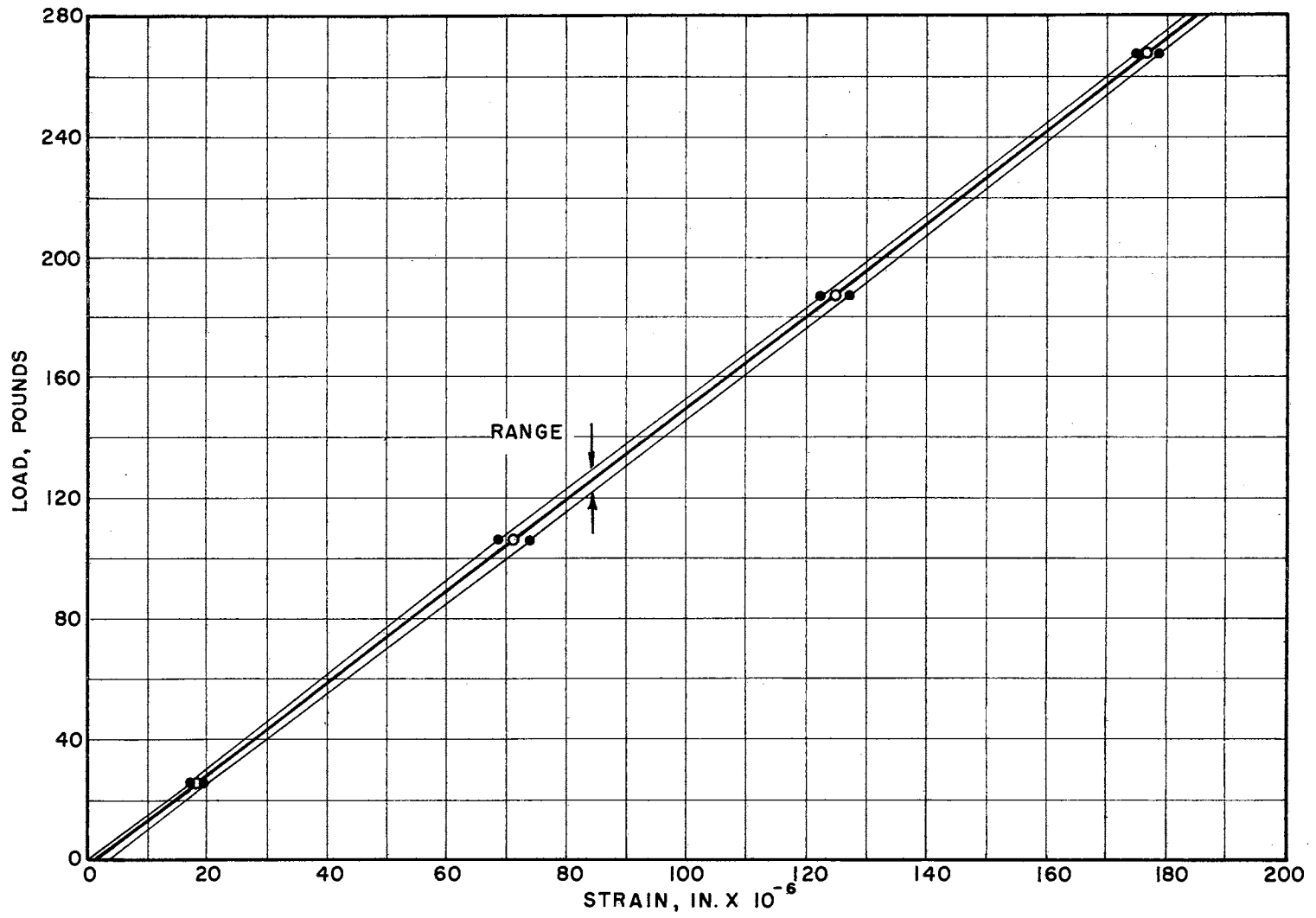
FIGURE 13
CALIBRATION CURVE FOR GAUGE 2S1 AND 2S2. (PILE NO. 3)
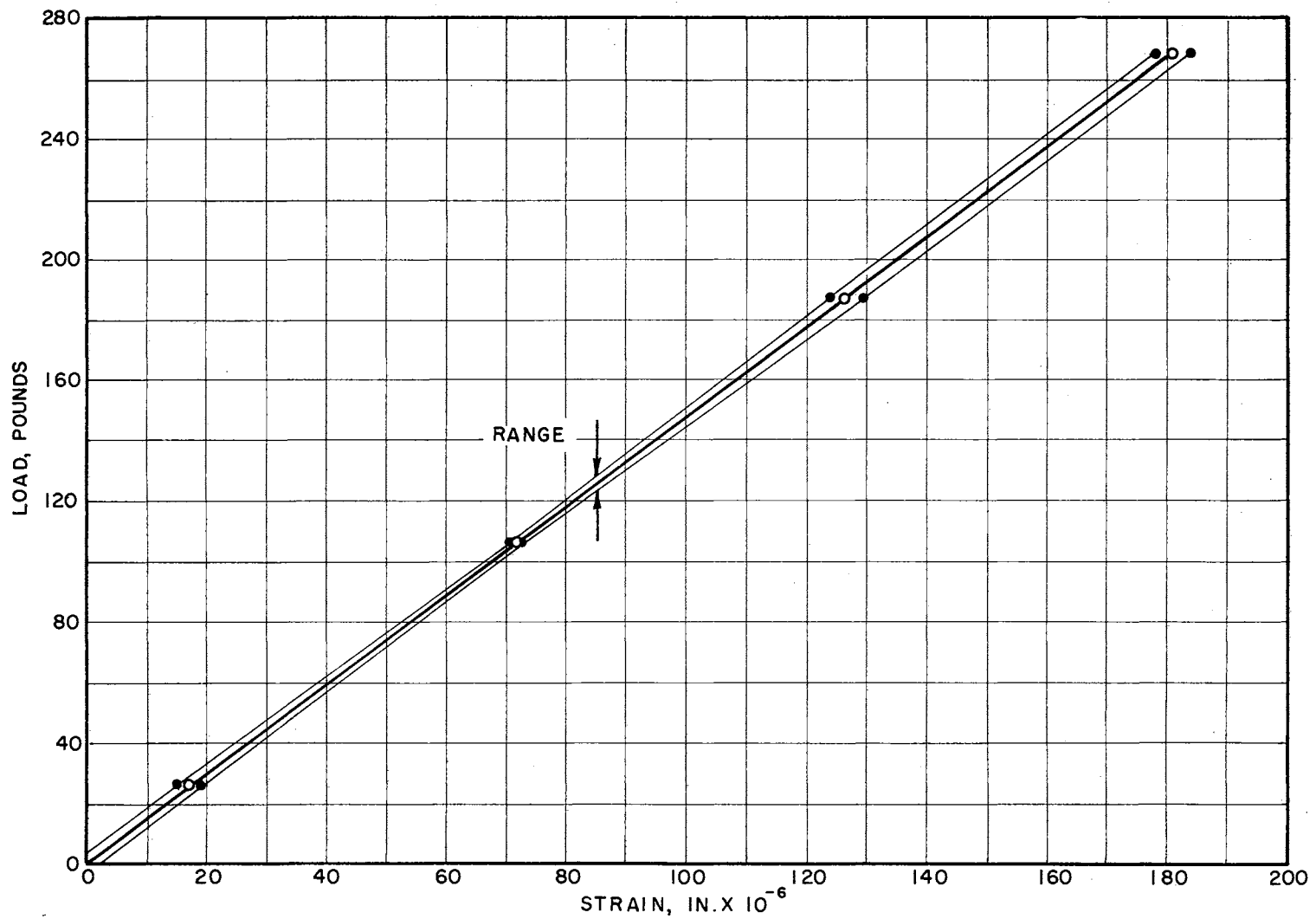
FIGURE 14

CALIBRATION CURVE FOR GAUGE 3SI AND 3S2. (PILE NO. 3)
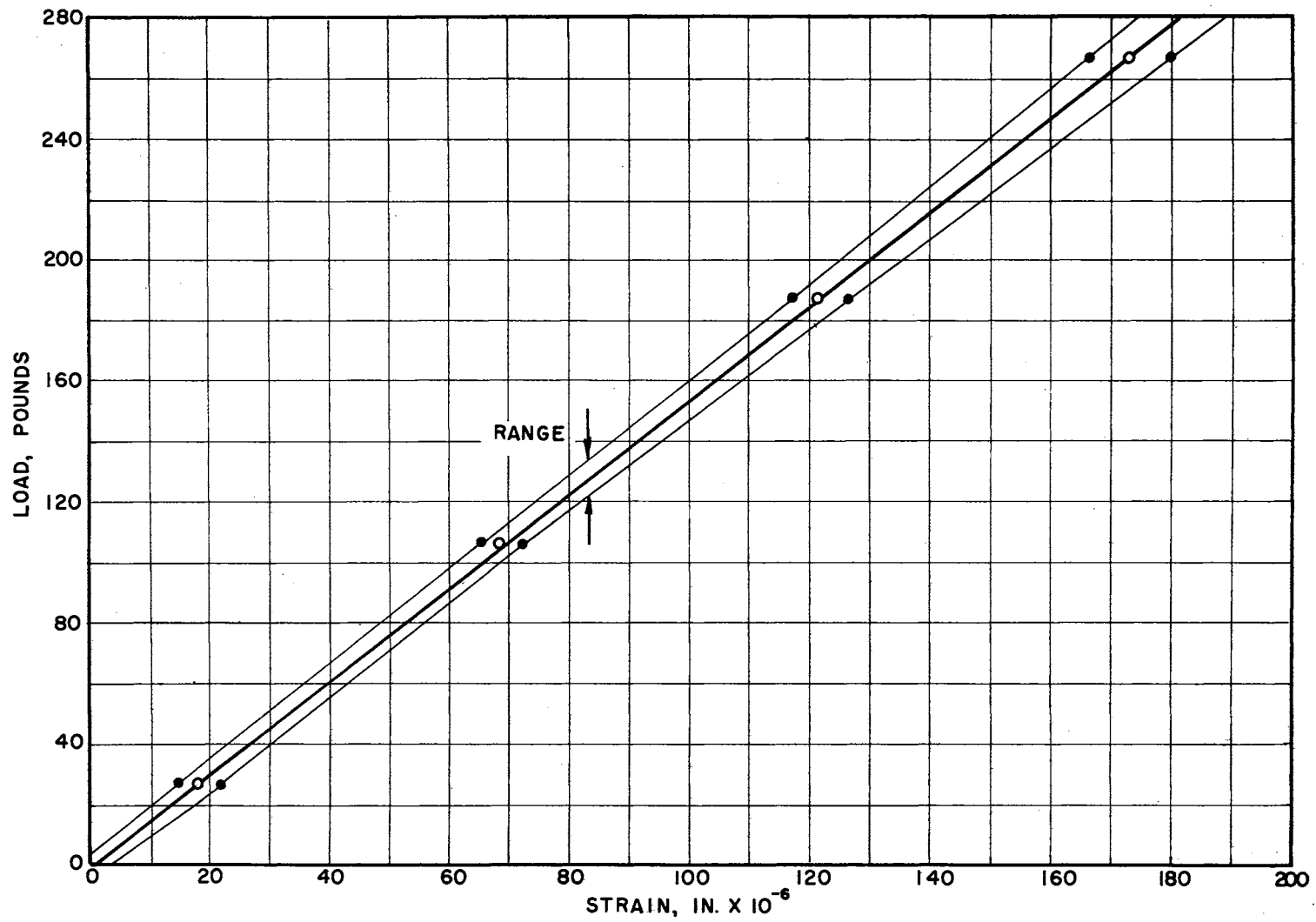
FIGURE 15

CALIBRATION CURVE FOR GAUGE 4SI AND 4S2.(PILE NO. 3)
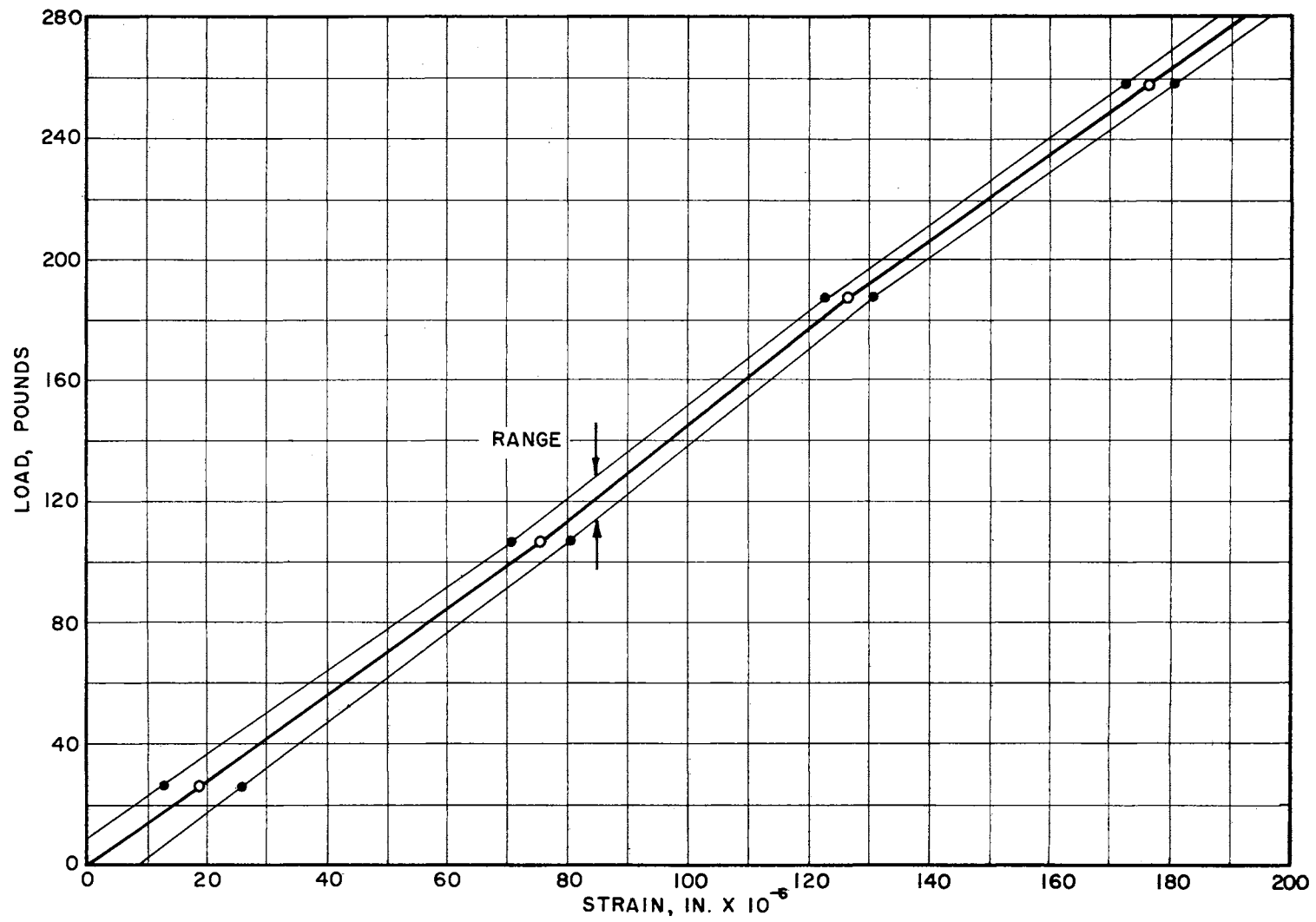
FIGURE 16
CALIBRATION CURVE FOR GAUGE 5S1 AND 5S2. (PILE NO.3)

to a height of 20 inches. The average relative density of the sand sample was 0.38.

Layered Soil

A layered sample of soil composed of an 8.0 inch thick clay layer on top of a 12.0 inch sand layer was prepared in a container 14.0 inches in diameter. The properties of the two types of soil used was as in the two previous samples.

Test Procedure

Each pile was driven into the soil by a 0.655 lb. drop hammer having a free fall of 6.0 inches. Driving was terminated when the total depth of penetration was 16.0 inches, thus one pair of strain gauges was left above the elevation of the soil surface. This was done with the intention of checking the load computed from the readings of these gauges with the actual load applied to the pile. A dial gauge, reading to the nearest .0001 of an inch, was utilized for the determination of the settlement of the pile top under the influence of the applied test load. An initial zero reading was recorded for the dial and all the strain gauges prior to the application of any load.

The test load was generally applied in increments, and each increment was maintained constant for a period just sufficient to record all the gauge readings. When the applied load reached the magnitude of half the full test load and when it reached the magnitude of the full test load, it was left applied to the pile for a period of 24 hours or until the settlement was less than 0.001 of an inch per hour.

The dial and strain gauge readings were recorded immediately after the application of these loads and immediately prior to their changes. In addition to the two terminal values, several readings were recorded during the period each of these two loads was maintained. This procedure was repeated for some of the piles in the different types of soil samples. Plate III shows a model pile during a load test.
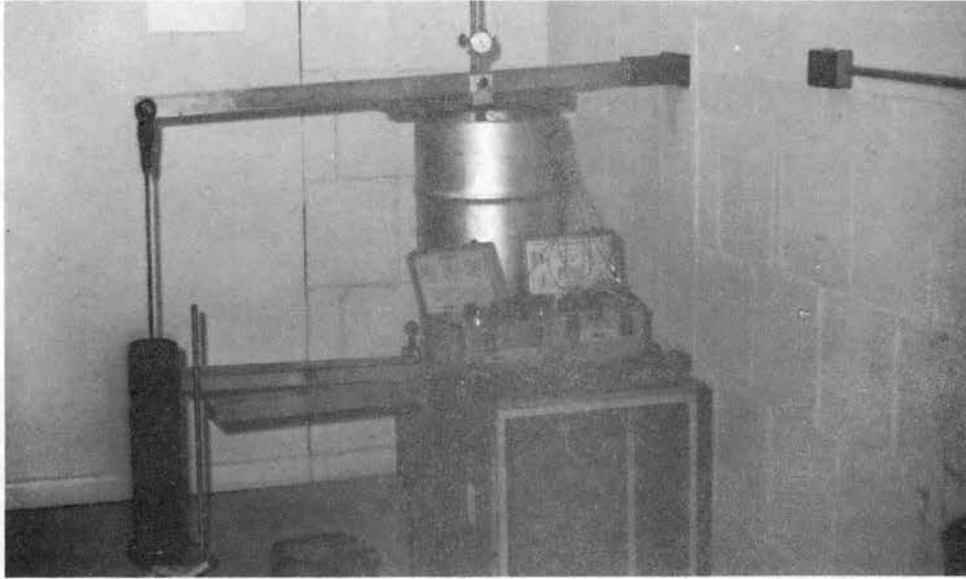
(a)
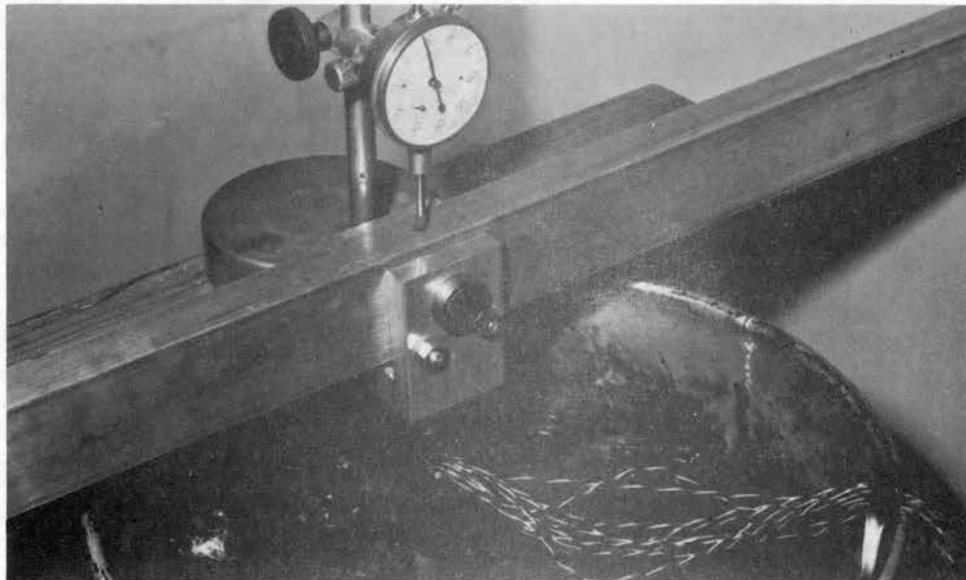
(b)

PLATE 3

MODEL PILE DURING LOADING TEST

CHAPTER III

TEST RESULTS

Strain Gauge Readings

Problems involving the shift of the null-balance point of the indicator dial in the reading instrument indicating drift with time of the strain readings reduced the scope of the investigation and restricted the possibilities of investigating the possible redistribution of stresses along the pile under sustained load for a long interval of time. Theoretically the readings of the galvanometer needle should remain at zero indefinitely if the bridge was balanced and the condition of the test kept constant. The drift was indicated by the change in strain readings for the upper pair of gauges, which were above the soil surface, and also by the highly erratic indications of strains by the rest of the gauges, under a sustained load for a period of 24 hours. The factors which can cause drift are:

1. Incomplete temperature compensation of the active strain gauges.

2. Improperly bonded strain gauges.

3. Creep of one or more strain gauges.

4. Instability of reading instrument.

5. Variations in the impedance of the lead wires.

6. Reduction in the impedance between the gauge filament, or lead wires and ground.

However, factor two was thought to be ineffective in this case due to

31

the fact that the probability of having thirty improperly bonded strain gauges was minute. The rest of the factors could have contributed to the instability of the system. These factors, especially one and three, were beyond the scope of the investigation and thus the investigation was limited to the study of the variation of stress along the model piles as the load applied at the top of the pile is increased during a short period of time. However the test load was left on some of the model piles during the course of the investigation with the hope of obtaining some logical readings of the strains along the piles under the sustained load after a period of time. Unfortunately, the results of the sustained load tests were erratic and seemed to have little value, if any. Aside from the problems associated with drift, the calibration curves of the strain gauges presented in Figures 3 through 16 indicated the existence of a probable error, associated with each reading, which varies from a minimum of six pounds for gauge 1S1 and 1S2, pile 3 Figure 12 to a maximum of about forty pounds for gauge 2S1 and 2S2, pile 2 Figure 9. Thus the loads presented in the Load Distribution Figures were only one among a number of possible values within the range of the calibration curve for each pair of strain gauges. However, it is believed that the trends indicated in the Load Distribution Figures are reasonable and logical and fairly represent the data collected.

<div align="center">Load Distribution on Model Piles in Sand</div>

Tables 2, 3, and 4 present the recorded values of the strain gauge readings together with the valves of the vertical deflection for

<div align="center">

TABLE 2

Load Distribution for Pile 1 in Sand

</div>

Load at Pan lbs	Load at Pile lbs	Gauge 1		Gauge 2		Gauge 3		Gauge 4		Gauge 5		Dial Reading in x 10^{-4}	Time
		1S1	1S2	2S1	2S2	3S1	3S2	4S1	4S2	5S1	5S2		
		−	−	−	−	−	+	+	−	−	−		
0	0	2577	0717	0891	1726	4492	7534	1978	3084	3762	4137	1000	11 p.m.
0	26.58	2589	0728	0903	1739	4511	7522	1952	3095	3792	4147	1150	
4.4	39.78	2595	0733	0912	1747	4522	7520	1947	3100	3806	4154	1195	
8.8	52.98	2602	0743	0925	1758	4536	7510	1934	3112	3821	4165	1254	
13.2	66.18	2612	0755	1937	1767	4545	7502	1926	3121	3832	4172	1332	
17.6	79.38	2620	0767	0947	1779	4555	7490	1916	3129	3843	4180	1470	
22.0	92.58	2627	0777	0960	1787	4563	7473	1909	3142	3854	4191	1865	
26.4	105.78	2633	0786	0962	1802	4559	7446	1922	3160	3859	4205	3930	12 p.m.
26.4	105.78	2763	0919	1100	1932	4697	7332	1793	3302	4947	4343	4085	10 p.m.

TABLE 3

Load Distribution for Pile 2 in Sand

Load at Pan lbs	Load at Pile lbs	Gauge 1		Gauge 2		Gauge 3		Gauge 4		Gauge 5		Dial Reading in x 10⁻⁴	Time
		1S1	1S2	2S1	2S2	3S1	3S2	4S1	4S2	5S1	5S2		
0	0	4823	4173	5928	3109	5657	2295	4172	1696	Damaged		3000	
0	26.58	4833	4185	5942	3125	5681	2301	4212	1690	during		3140	
4.4	39.78	4842	4196	5953	3134	5690	2307	4219	1702	Calibration		3210	
8.8	52.98	4852	4203	5965	3139	5699	2314	4225	1714			3263	
13.2	66.18	4859	4213	5972	3148	5709	2320	4238	1724			3344	
17.6	79.38	4867	4220	5980	3154	5725	2319	4240	1739			3480	
22.0	92.58	4877	4230	5999	3173	5737	2373	4250	1749			3880	
26.4	105.78	4888	4241	6012	3179	5752	2335	4262	1755			6000	

TABLE 4

Load Distribution for Pile 3 in Sand

Load at Pan lbs	Load at Pile lbs	Gauge 1		Gauge 2		Gauge 3		Gauge 4		Gauge 5		Dial Reading in x 10^{-4}	Time
		1S1	1S2	2S1	2S2	3S1	3S2	4S1	4S2	5S1	5S2		
		−	−	−	+	−	+	−	−	+	−		
0	0	1157	4734	3853	2457	5079	0119	3026	4473	4867	2308	2000	
0	26.58	1166	4743	3865	2445	5097	0109	3051	4482	4831	2318	2140	
4.4	39.78	1176	4753	3873	2437	5112	0106	3064	4485	4819	2323	2190	
8.8	52.98	1185	4762	3882	2428	5121	0101	3075	4492	4810	2331	2260	
13.2	66.18	1197	4774	3892	2418	5135	0095	3086	4499	4808	2338	2340	
17.6	79.38	1208	4785	3905	2405	5213	0091	3099	4504	4783	2344	2480	
22.0	92.58	1219	4796	3912	2398	5221	0081	3110	4513	4777	2752	2900	
26.4	105.78	1230	4807	3926	2384	5235	0075	3116	4523	4769	2360	5770	

each increment of loading. Figures 17, 18, and 19 illustrate the Load Distribution along the length of embedment for piles 1, 2, and 3, respectively, for the indicated values of the load increments. There is good agreement between the curves for the three piles for each increment of loading. The rate at which the load was being transferred from the pile to the sand at any depth is reflected by the slopes of these curves, which measure directly the frictional resistance which has been developed at that point. Closer study of the slopes of the curves indicate that the frictional resistance is rather uniform with depth. However there is only a slight increase from the lower third of the pile downward.

For the first four increments of the test load about one-fourth of the applied load was transferred to the soil at a uniform rate by friction along the circumferential area of the pile. The rest of the applied load was carried by point bearing at the tip. As the applied load increased the frictional resistance along the pile nearly disappeared along the upper part of the pile, as indicated by the almost vertical slope of that part of the curves. The load was almost exclusively carried by the lower part of the pile and by point bearing. Point bearing was almost ninety percent of the total applied load. As the applied load increased the pile failed by continuous movement into the sand. The strain recorded along the length of the pile during its movement downward indicated that most of the total applied load was acting at the tip, with only a small part being transferred to the adjacent surrounding sand along the pile due to sliding friction.

Figure 20 shows the vertical deflection under the increments
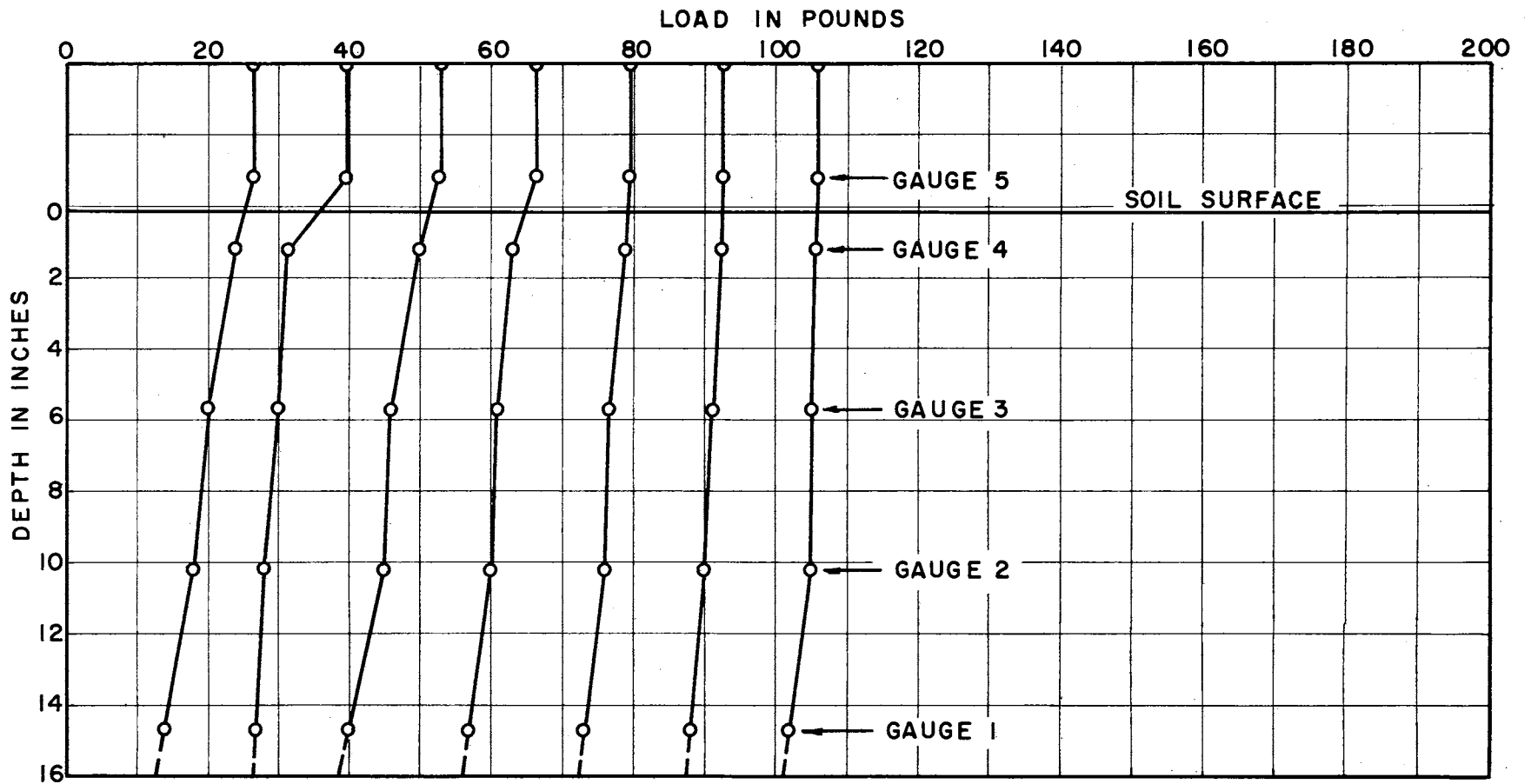
FIGURE 17

LOAD DISTRIBUTION FOR PILE NO. 1 IN SAND.
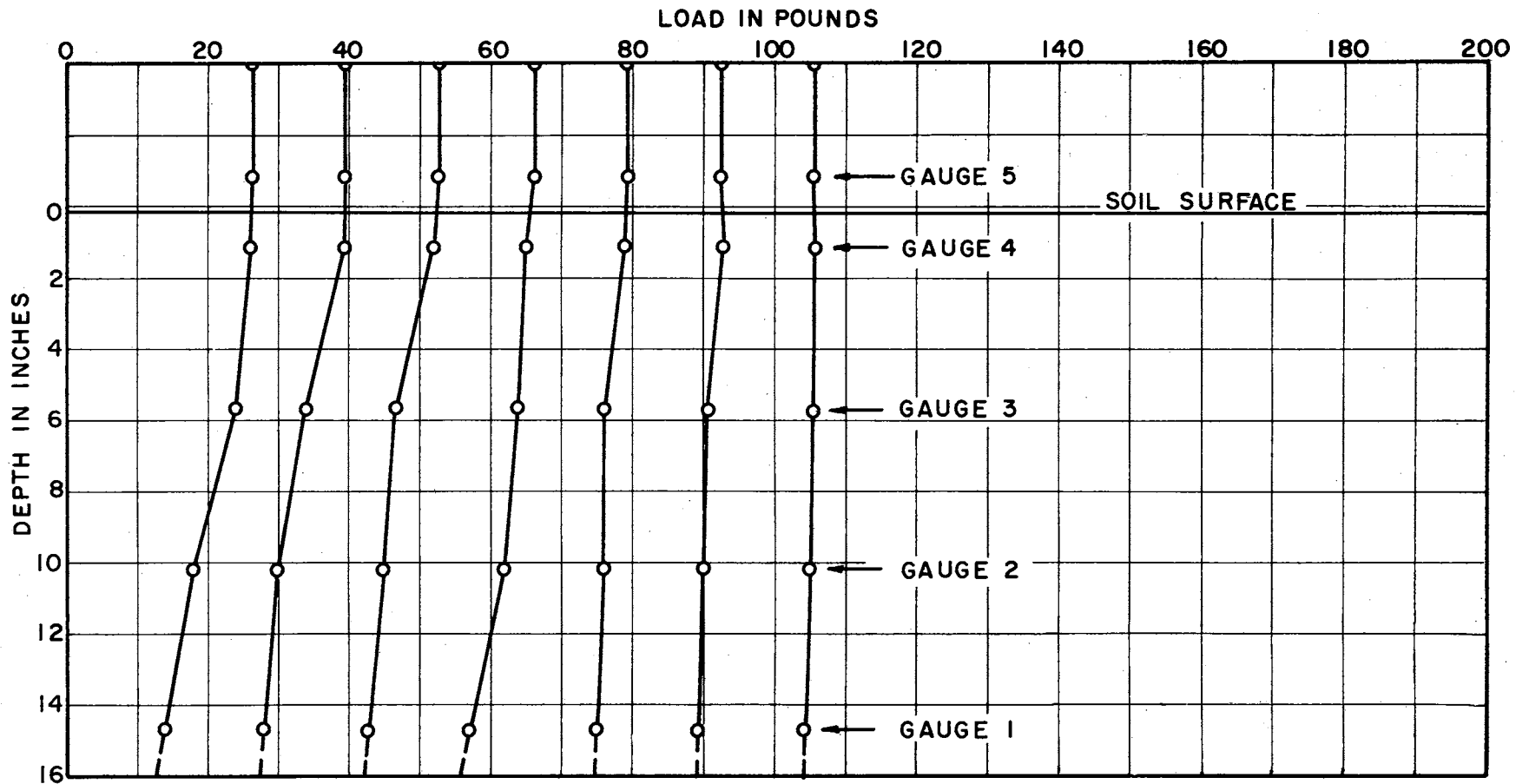
FIGURE 18

LOAD DISTRIBUTION FOR PILE NO. 2 IN SAND

LOAD IN POUNDS
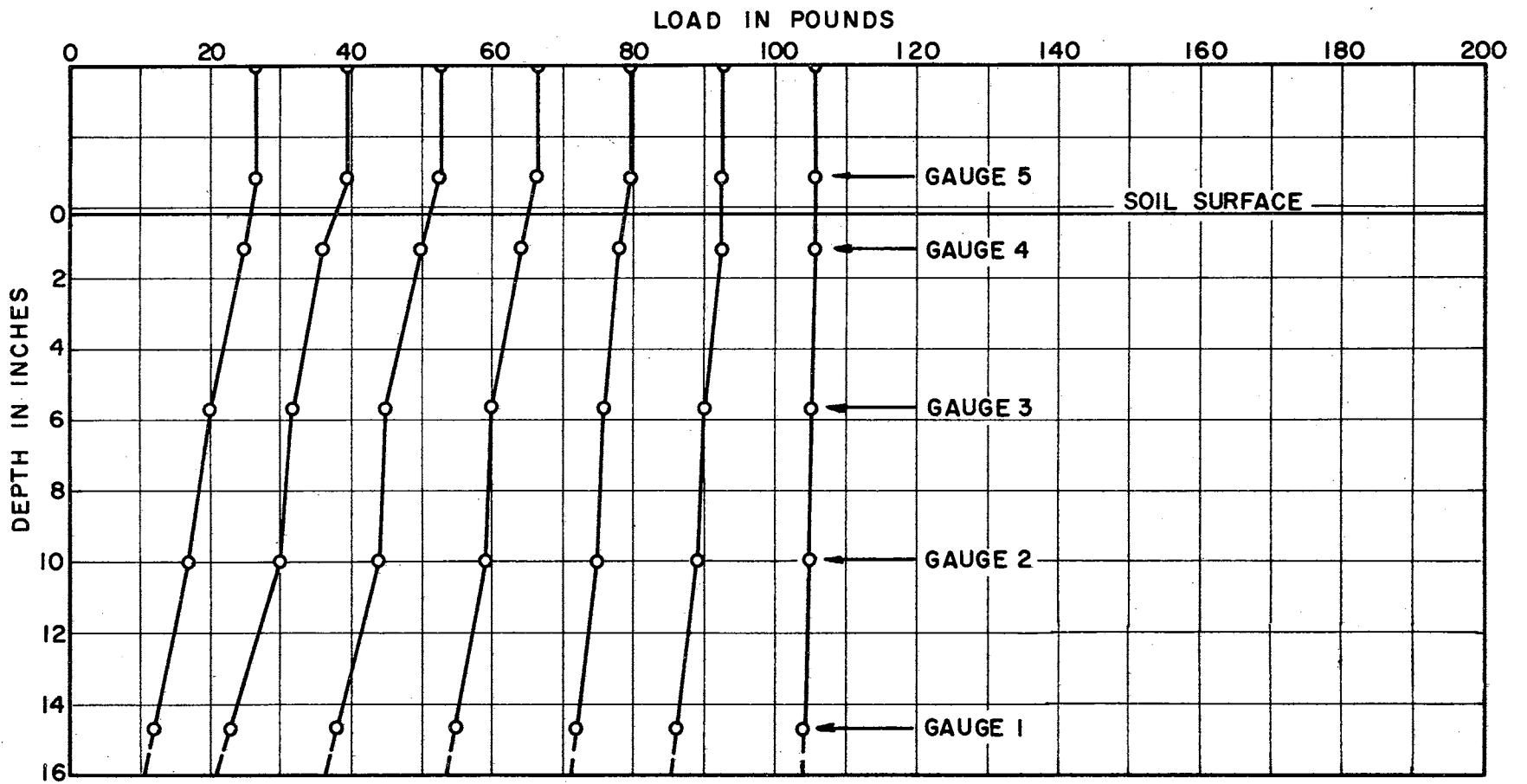
FIGURE 19

LOAD DISTRIBUTION FOR PILE NO. 3 IN SAND.
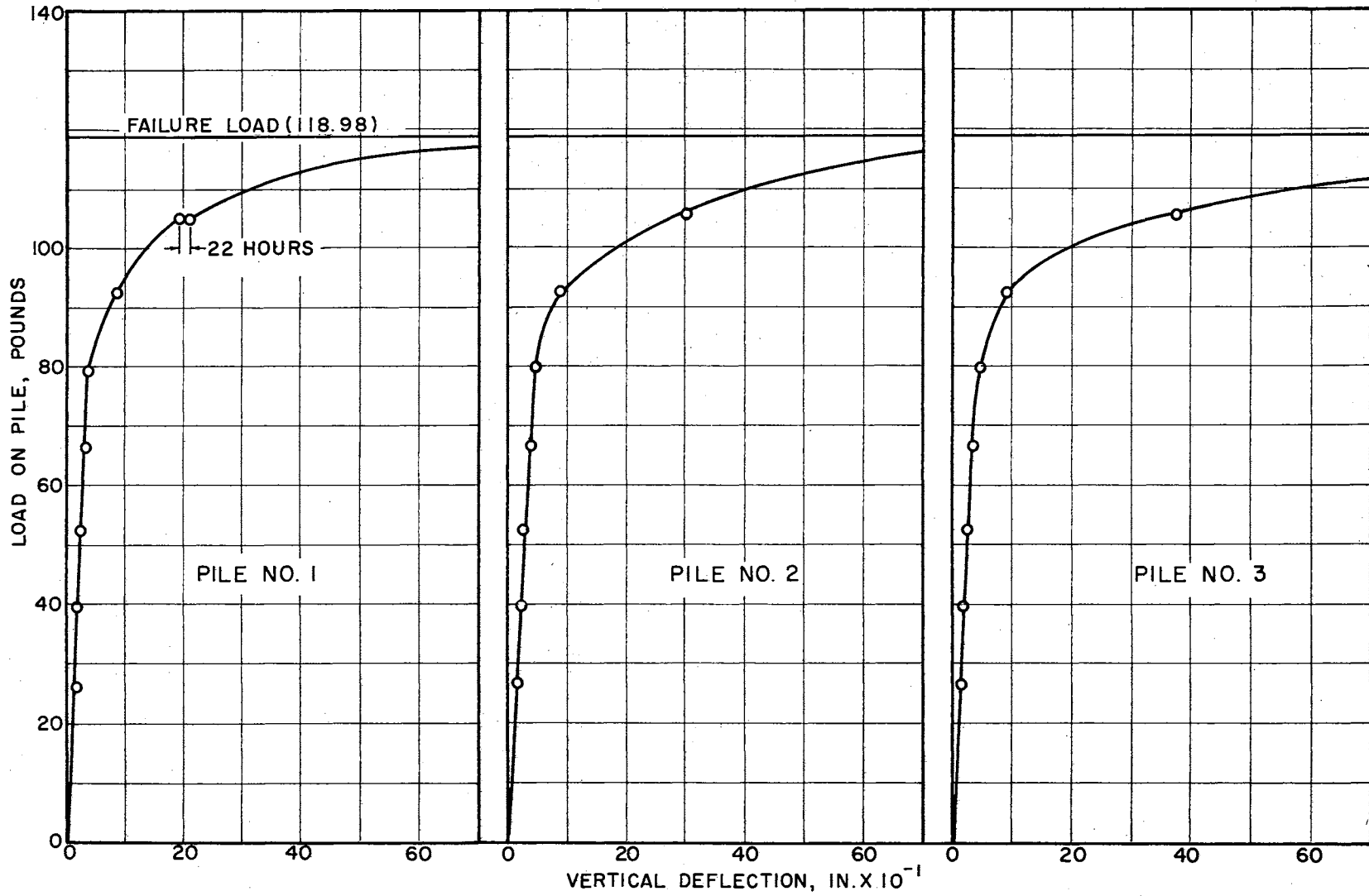
FIGURE 20
VERTICAL DEFLECTION UNDER LOAD IN SAND

of the test load for each pile. The three curves show good agreement
and indicate that there was almost a linear relation between the applied
load and the vertical deflection up to about eighty-five percent of the
total load. Thereafter, the sharp decrease in the slope indicated
that there was an appreciable vertical deflection with small incre-
ments of loading. The curves also indicated that there was little
vertical deflection up to about eighty-five percent of the total load
at failure.

Load Distribution on Model Piles in Clay

Tables 5, 6, and 7 present the recorded values of the strain
gauge readings together with the amount of vertical deflection for
each increment of loading. Figures 21, 22, and 23 illustrate the
load distribution along the length of embedment for piles 1, 2, and
3, respectively, for the indicated values of the load increments. A
comparison of Tables 5, 6, and 7 with these figures show that not all
of the applied load increments were represented in the figures. This
was due to the fact that an arbitrary chosen load was left, without
alteration, acting on the pile in an attempt to investigate the redistri-
bution, if any, of stresses along the pile with time; but the readings
obtained were erratic and of such nature that their inclusion as a
part of the analysis could not be justified from a statistical viewpoint.
However, three possible readings for the lower three strain gauges
of pile 2 were plotted in Figure 22 indicating a redistribution of stress
with time, during which more load is transmitted to the lower part
of the pile as indicated by the higher values of loads and the flatter

TABLE 5

Load Distribution for Pile 1 in Clay

Load at Pan lbs	Load at Pile lbs	Gauge 1		Gauge 2		Gauge 3		Gauge 4		Gauge 5		Dial Reading in x 10^{-4}	Time
		1S1	1S2	2S1	2S2	3S1	3S2	4S1	4S2	5S1	5S2		
		−	−	−	−	−	+	−	−	−	−		
0	0	5615	4302	4779	5058	7312	0858	2675	6447	6553	6669	1000	11 p.m.
0	26.58	5618	4305	4785	5065	7317	0849	2671	6487	6548	6710	1039	
4.4	39.78	5618	4303	4784	5066	7320	0844	2673	6504	6550	6727	1052	
8.8	52.98	5619	4305	4786	5069	7324	0839	2671	6517	6550	6741	1065	
13.2	66.18	5619	4305	4787	5071	7327	0835	2677	6527	6553	6755	1078	
17.6	79.38	5619	4305	4788	5073	7332	0829	2687	6535	6559	6769	1089	
22.0	92.58	5619	4305	4789	5075	7333	0824	2690	6542	6566	6782	1099	
26.4	105.78	5619	4305	4792	5079	7340	0818	2703	6551	6575	6795	1105	
30.8	118.98	5621	4307	4795	5083	7345	0813	2709	6559	6580	6810	1115	
32.2	132.18	5621	4307	4795	5084	7347	0810	2717	6565	6589	6821	1125	
39.6	145.38	5621	4307	4796	5087	7353	0803	2726	6575	6598	6838	1131	
44.0	158.58	5621	4307	4799	5089	7356	0799	2734	6581	6604	6850	1140	
48.4	171.78	5622	4308	4801	5093	7361	0794	2743	6587	6611	6861	1147	
52.8	184.98	5621	4305	4800	5093	7363	0791	2749	6594	6618	6877	1154	
57.2	198.18	5623	4310	4803	5098	7373	0787	2758	6600	6625	6886	1162	

TABLE 6

Load Distribution for Pile 2 in Clay

Load at Pan lbs	Load at Pile lbs	Gauge 1		Gauge 2		Gauge 3		Gauge 4		Gauge 5		Dial Reading in x 10^{-4}	Time
		1S1	1S2	2S1	2S2	3S1	3S2	4S1	4S2	5S1	5S2		
		−	−	−	−	−	−	−	+				
0	0	7719	7038	8773	6038	8512	5216	7037	4468			2000	11 p.m.
0	26.58	7721	7042	8780	6043	8523	5227	7071	4476			2031	
4.4	39.78	7721	7042	8779	6046	8525	5227	7082	4478			2045	
8.8	52.98	7723	7042	8783	6048	8529	5232	7096	4479			2057	
13.2	66.18	7724	7043	8786	6051	8536	5238	7108	4487			2070	
17.6	79.38	7726	7045	8791	6055	8543	5223	7119	4497			2080	
22.0	92.58	7725	7043	8791	6056	8547	5247	7127	4493			2090	
26.4	105.78	7724	7045	8793	6058	8553	5253	7139	4500			2100	
30.8	118.98	7727	7047	8801	6067	8561	5259	7145	4505			2110	
30.8	118.98	7737	7053	8850	6070	8617	5221	6888	3673			2142	11 p.m.
35.2	132.18	7740	7055	8857	6076	8623	5227	6894	3697			2148	
39.6	145.38	7741	7055	8862	6077	8625	5230	6902	3703			2157	

TABLE 7

Load Distribution for Pile 3 in Clay

Load at Pan lbs	Load at Pile lbs	Gauge 1		Gauge 2		Gauge 3		Gauge 4		Gauge 5		Dial Reading in x 10^{-4}	Time
		1S1 −	1S2 −	2S1 −	2S2 −	3S1 −	3S2 −	4S1 −	4S2 −	5S1 +	5S2 −		
0	0	8962	5328	7863	1533	9397	3954	7227	8740	1383	6491	2000	2:40 p.m.
0	26.58	8962	5328	7869	1537	9404	3963	7249	8748	1362	6496	2045	
4.4	39.78	8964	5330	7872	1539	9408	3965	7263	8750	1347	6500	2054	
8.8	52.98	8967	5334	7878	1543	9416	3974	7281	8752	1332	6505	2080	
13.2	66.18	8971	5334	7882	1548	9423	3979	7297	8754	1317	6510	2095	
17.6	79.38	8977	5342	7892	1558	9439	3993	7325	8758	1293	6516	2110	3:05 p.m.
17.6	79.38	9119	5469	7989	1641	9572	4008	7261	8641	1402	6629	2111	10:00 p.m.
17.6	79.38	9302	5541	7985	1509	9693	3703	10557	8466	0902	6621	2110	10:00 a.m.
17.6	79.38	9382	5540	7960	1384	9732	3559	10849	8486	1830	6660	2089	3:05 p.m.
22.0	92.58	9385	5542	7960	1384	9736	3555	10817	8493	1828	6669	2098	
26.4	105.78	9390	5542	7962	1384	9742	3558	10835	8503	1822	6673	2108	
30.8	118.98	9398	5548	7963	1382	9742	3558	10838	8513	1822	6682	2118	
35.2	132.18	9399	5546	7967	1382	9751	3562	10871	8522	1820	6689	2128	
39.6	145.38	9400	5547	7971	1384	9753	3567	10879	8531	1815	6695	2137	
44.0	158.58	9402	5547	7972	1382	9760	3564	10902	8538	1810	6708	2145	3:30 p.m.
44.0	158.58	9470	5317	7723	0700	9800	2932	11179	8508	1245	6746	2160	11:15 a.m.
48.4	171.78	9479	5319	7725	0700	9803	2933	10099	8519	1221	6759	2167	

TABLE 7 (Cont.)

Load at Pan lbs	Load at Pile lbs	Gauge 1		Gauge 2		Gauge 3		Gauge 4		Gauge 5		Dial Reading in x 10^{-4}	Time
		1S1	1S2	2S1	2S2	3S1	3S2	4S1	4S2	5S1	5S2		
52.8	184.98	9485	5322	7727	0701	9809	2937	10070	8533	1210	6770	2174	
57.2	198.18	9480	5320	7725	0700	9810	2937	10042	8543	1205	6785	2181	
61.6	211.38	9480	5320	7725	0695	9813	2935	10062	8553	1193	6794	2189	

LOAD IN POUNDS
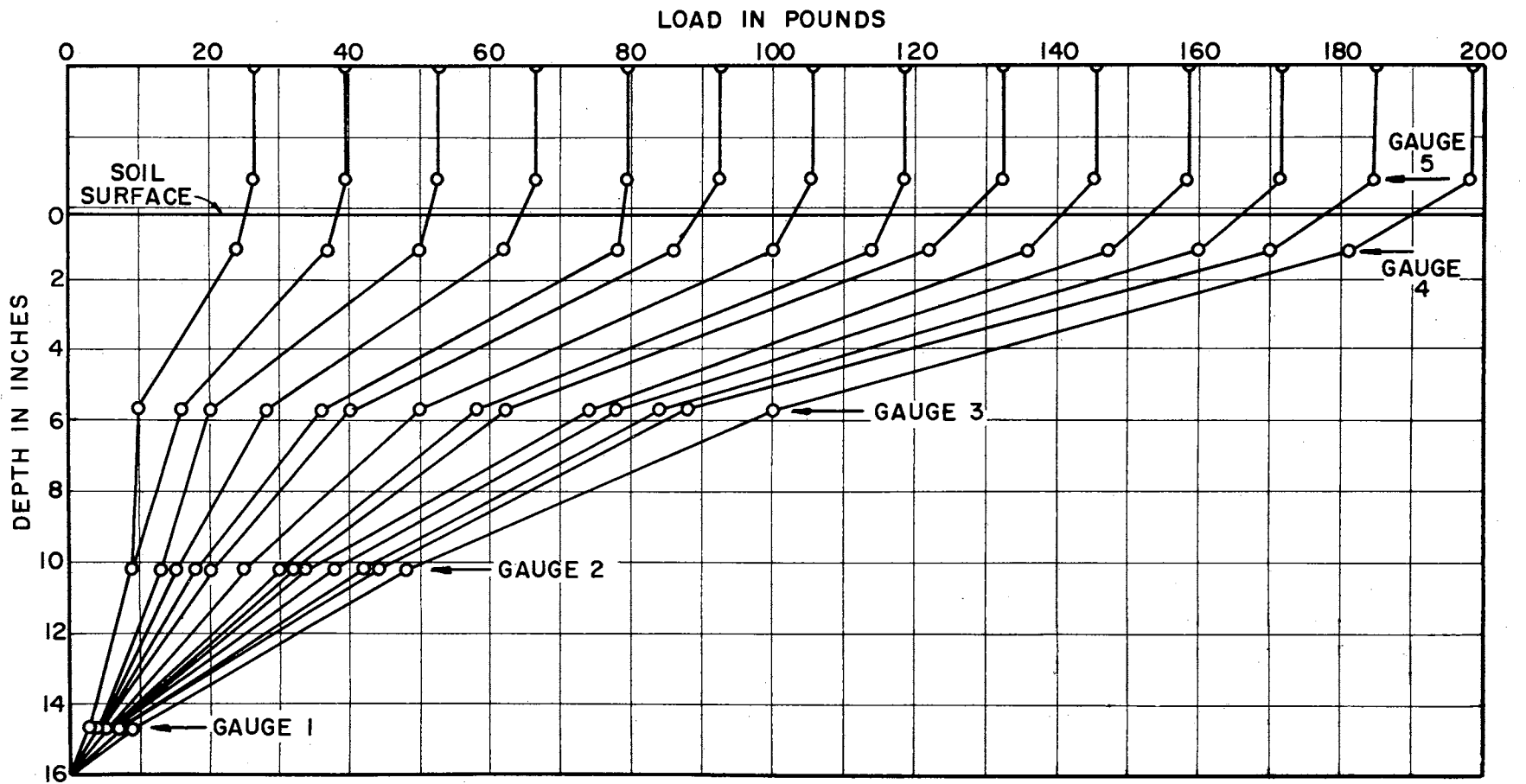
FIGURE 21

LOAD DISTRIBUTION FOR PILE NO. 1 IN CLAY.
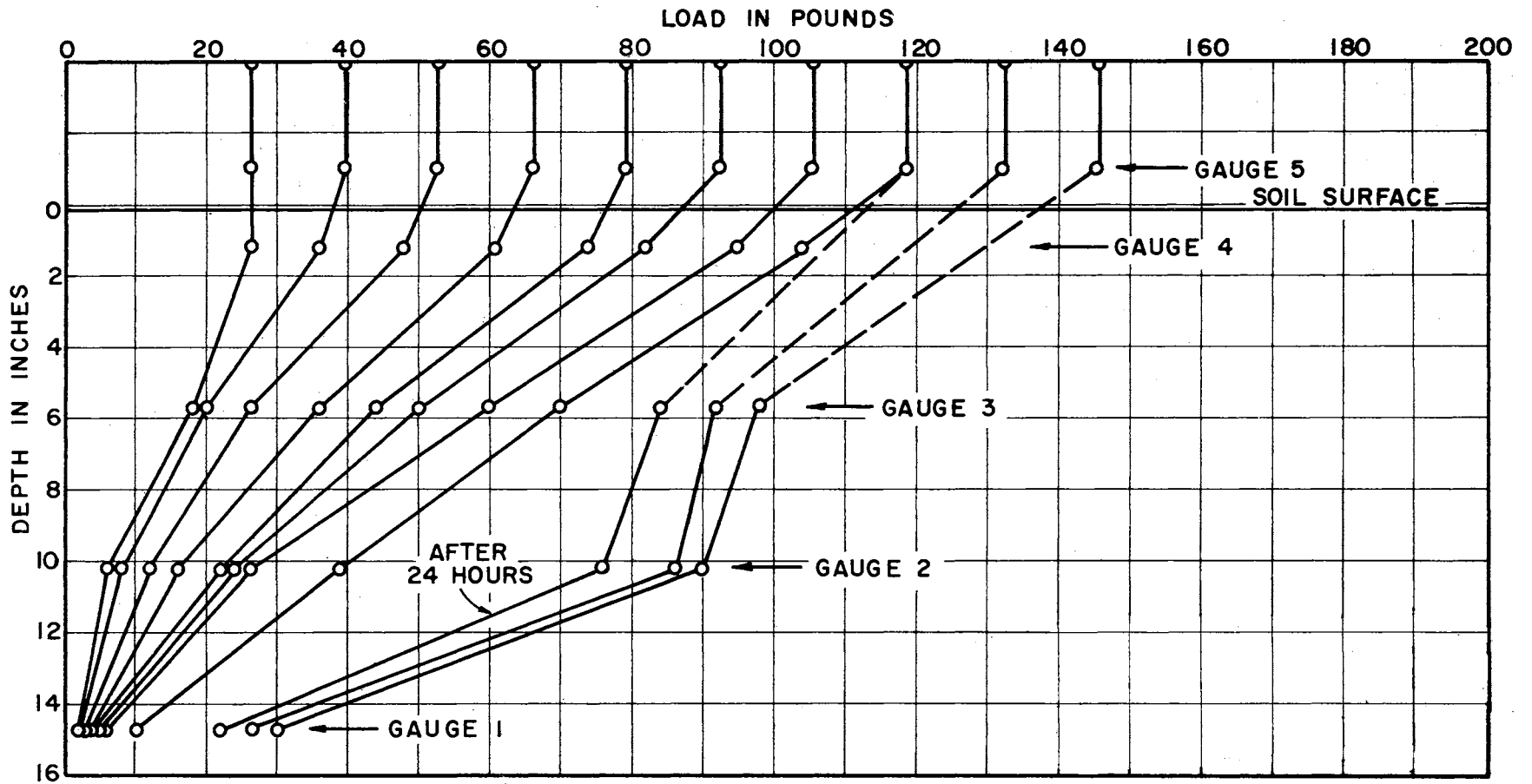
FIGURE 22

LOAD DISTRIBUTION FOR PILE NO. 2 IN CLAY
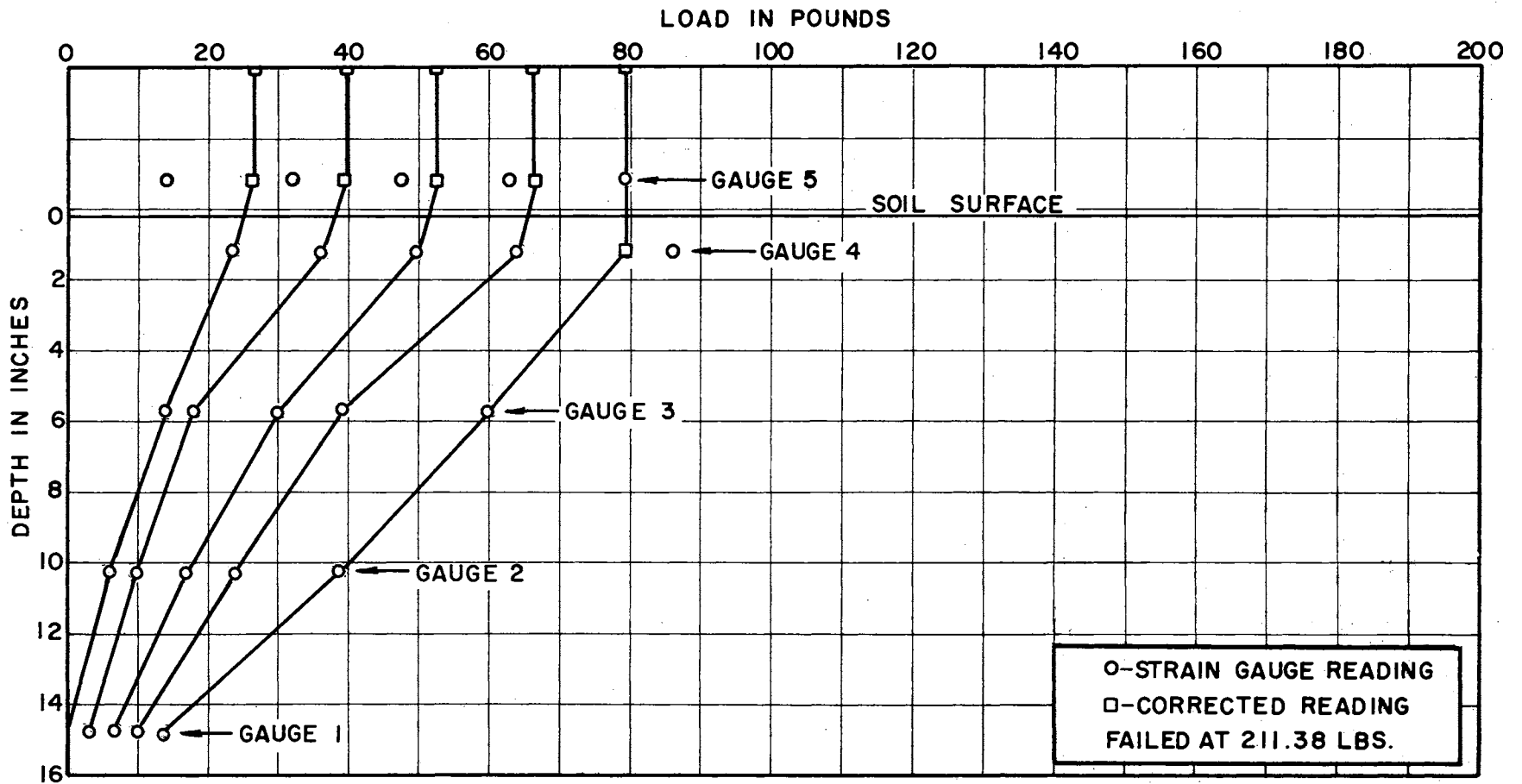
FIGURE 23

LOAD DISTRIBUTION FOR PILE NO. 3 IN CLAY

slopes of the curves at this region.

An examination of Figures 21, 22, and 23 shows that the load transmitted to the soil for each load increment is greatest along the upper third of the piles. This is indicated by the flatter slopes of the upper part of each curve. As the applied load increased the slope of the upper third of the load distribution along the pile decreased, indicating that the percentage of load transmitted at this section had increased. The figures also show that the load at or near the tip is very small and that it does not increase appreciably with the increase of load. The remaining load at the lower quarter point of the embedded length of the pile was about five percent of the total applied load, indicating that about ninety-five percent of the load had been transferred to the soil.

The strain readings for gauges 5 and 4 on pile 3 gave erroneous readings which did not agree with the applied load. These were corrected as indicated in Figure 23.

Figure 24, which shows the vertical deflection of each pile under the increments of loading, indicates that piles 1 and 3 had almost identical ultimate capacities of about 220 pounds and that pile 2 failed at a load of about 160 pounds. This lower ultimate capacity could be attributed to the break of bondage between the two halves of pile 2 during either driving or testing. The breakage of the bond was discovered when the piles were examined after the test.

The slopes of the vertical deflection curves for the piles, presented in Figure 24, show that the clay soil experienced little strain with increased applied load on the pile. The steep uniform
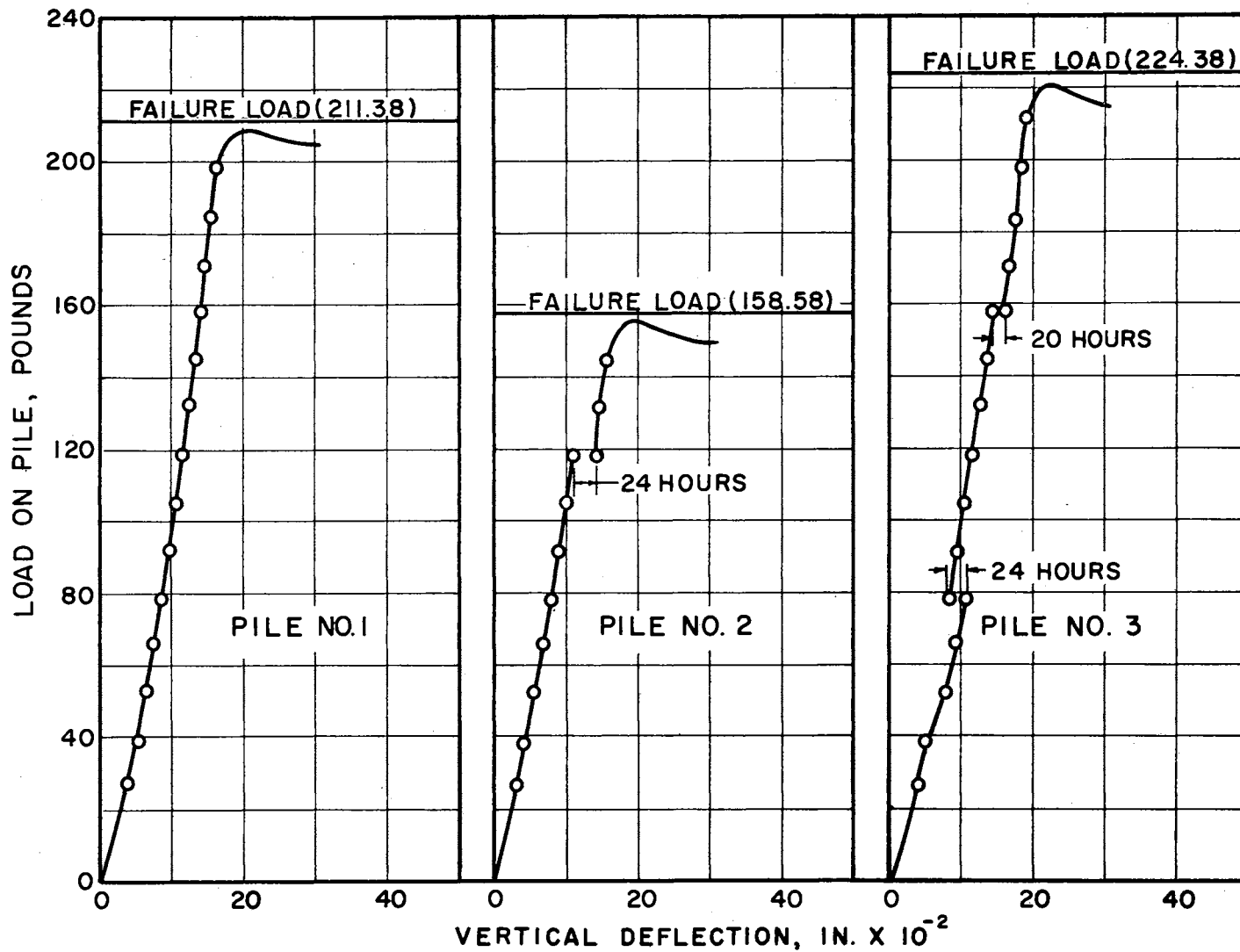
FIGURE 24

VERTICAL DEFLECTION UNDER LOAD IN CLAY

slopes and final plunging into the soil as failure occurred indicate that the failure of the piles under the maximum applied load occurred because the test load was greater than the ultimate adhesion between the pile and the clay soil. This was confirmed by the absence, around the pile, of surface shear cracks which should have existed if the failure was due to shear failure in the soil.

The recorded strains during failure of the pile indicated that there was appreciable load transferred to the adjacent clay soil along the whole length of the pile due to sliding friction.

Another phenomenon which is thought to be of some importance was that the pile carried the maximum applied load for a few seconds before it failed which indicated the possibility of progressive failure. A progressive type of failure is consistent with the existence of non-uniform stress transfer conditions such as were observed in all of these piles. Apparently, the adhesive strength is first reached and exceeded along the upper part of the pile, resulting in a transfer of stress downward toward the pile tip as the strength is progressively overcome on the section above. The time needed for this phenomenon probably reflects the specific strength properties of the soil and the magnitude of the final load increment.

Load Distribution on Model Piles in Layered Soil

Tables 8, 9, and 10 record the values of the strain gauge readings together with the values of the vertical deflection for each increment of loading. Figures 25, 26, and 27 illustrate the load distribution along the length of piles 1, 2, and 3, respectively, for

TABLE 8

Load Distribution for Pile 1 in Layered Soil

Load at Pan lbs	Load at Pile lbs	Gauge 1		Gauge 2		Gauge 3		Gauge 4		Gauge 5		Dial Reading in x 10⁻⁴	Time
		1S1	1S2	2S1	2S2	3S1	3S2	4S1	4S2	5S1	5S2		
		$-$	$-$	$-$	$-$	$-$	$+$	$+$	$-$	$-$	$-$		
0	0	3317	1434	1623	2417	5261	7060	1222	3837	4507	4843	1000	3:15 p.m.
0	26.58	3320	1439	1630	2423	5270	7048	1217	3861	4521	4860	1053	
4.4	39.78	3321	1441	1632	2428	5276	7047	1203	3868	4531	4863	1067	
8.8	52.98	3325	1445	1639	2432	5282	7041	1183	3873	4551	4875	1085	
13.2	66.18	3329	1448	1643	2439	5288	7039	1179	3883	4562	4885	1098	
17.6	79.38	3331	1449	1645	2441	5297	7035	1169	3895	4575	4898	1105	
22.0	92.58	3332	1450	1648	2443	5300	7031	1157	3901	4583	4903	1113	
26.4	105.78	3334	1453	1652	2447	5303	7026	1146	3909	4596	4909	1122	
30.8	118.98	3335	1453	1655	2449	5311	7023	1132	3912	4610	4913	1129	
35.2	132.18	3337	1456	1659	2450	5313	7021	1123	3919	4621	4920	1137	
39.6	145.38	3337	1456	1659	2451	5318	7014	1113	3923	4633	4927	1145	
44.0	158.58	3340	1460	1663	2453	5327	7009	1103	3925	4643	4929	1155	
48.4	171.78	3360	1477	1686	2476	5348	6991	1094	3935	4654	4937	1258	
48.4	171.78	3299	1286	1721	2419	5382	7055	1132	3861	4628	4925	1265	9:40 a.m.
52.8	184.98	3302	1289	1722	2422	5387	7051	1115	3863	4633	4930	1270	
57.2	198.18	3302	1289	1721	2419	5388	7051	1111	3869	4642	4943	1275	
61.6	211.38	3303	1291	1723	2422	5387	7050	1104	3875	4651	4948	1286	

TABLE 8 (Cont.)

Load at Pan lbs	Load at Pile lbs	Gauge 1		Gauge 2		Gauge 3		Gauge 4		Gauge 5		Dial Reading in x 10^{-4}	Time
		1S1	1S2	2S1	2S2	3S1	3S2	4S1	4S2	5S1	5S2		
66.0	224.58	3520	1305	1752	2440	5400	7039	1100	3849	4659	4944	2790	
66.0	224.58	3259	1073	1708	2364	5425	6982	0960	3870	4671	4960	2830	3:00 p.m.
70.4	237.78	3260	1075	1716	2365	5429	6675	0952	3872	4681	4970	2835	
74.8	250.98	3260	1073	1718	2361	5425	6683	0970	3873	4691	4977	2845	
79.2	264.18	3262	1073	1719	2363	5429	6657	1141	3883	4700	4981	6432	

TABLE 9

Load Distribution for Pile 2 in Layered Soil

Load at Pan lbs	Load at Pile lbs	Gauge 1		Gauge 2		Gauge 3		Gauge 4		Gauge 5		Dial Reading in x 10^{-4}	Time
		1S1	1S2	2S1	2S2	3S1	3S2	4S1	4S2	5S1	5S2		
		−	−	−	−	−	−	−	+				
0	0	4962	3598	5963	2622	5393	1658	0956	1415			1000	12 midnight
0	26.58	4963	3601	5970	2629	5403	1667	0973	1397			1115	
4.4	39.78	4963	3602	5971	2631	5409	1672	0981	1388			1137	
8.8	52.98	4967	3602	5978	2637	5413	1677	0992	1380			1152	
13.2	66.18	4970	3605	5983	2641	5420	1681	1000	1370			1165	
17.6	79.38	4973	3610	5989	2644	5427	1685	1006	1370			1181	
22.0	92.58	4975	3610	5993	2649	5431	1691	1015	1351			1192	
26.4	105.78	4979	3613	6001	2652	5439	1693	1024	1341			1204	
30.8	118.98	4983	3618	6008	2669	5449	1702	1034	1333			1219	
35.2	132.18	4987	3622	6016	2669	5457	1709	1047	1323			1232	
39.6	145.38	4997	3631	6023	2673	5467	1721	1057	1317			1250	
44.0	158.58	5005	3639	6037	2685	5479	1731	1069	1306			1270	
48.4	171.78	5013	3646	6049	2692	5489	1740	1078	1293			1301	
52.8	184.98	5022	3657	6058	2705	5499	1749	1093	1280			1360	
57.2	198.18	5028	3670	6071	2717	5509	1758	1089	1267			1452	
57.2	198.18	5002	3541	6917	2446	5633	1757	1323	0938			1475	10:30 p.m.
61.6	211.38	5004	3541	6929	2445	5641	1762	1331	0927			1482	

TABLE 9 (Cont.)

Load at Pan lbs	Load at Pile lbs	Gauge 1		Gauge 2		Gauge 3		Gauge 4		Gauge 5		Dial Reading in x 10^{-4}	Time
		1S1	1S2	2S1	2S2	3S1	3S2	4S1	4S2	5S1	5S2		
66.0	224.58	5004	3545	6935	2445	5643	1763	1335	0915			1491	
70.4	237.78	5008	3548	6949	2447	5649	1766	1338	0907			1503	
74.8	250.98	5015	3561	6963	2451	5631	1797	1351	0909			1880	

TABLE 10

Load Distribution for Pile 3 in Layered Soil

Load at Pan lbs	Load at Pile lbs	Gauge 1		Gauge 2		Gauge 3		Gauge 4		Gauge 5		Dial Reading in x 10^{-4}	Time
		1S1 −	1S2 −	2S1 −	2S2 −	3S1 −	3S2 −	4S1 −	4S2 −	5S1 +	5S2 −		
0	0	6864	3425	4860	5700	2310	5322	6420	1978	5612	3980	1000	
0	26.58	6871	3432	4870	5710	2324	5332	6438	1994	5582	4000	1065	
4.4	39.78	6872	3433	4872	5712	2331	5335	6446	2002	5574	4008	1085	
8.8	52.98	6875	3436	4878	5718	2336	5340	6460	2010	5569	4013	1103	
13.2	66.18	6880	3441	4882	5722	2342	5344	6468	2018	5657	4025	1118	
17.6	79.38	6885	3446	4886	5726	2347	5347	6478	2024	5549	4033	1135	
22.0	92.58	6888	3449	4890	5730	2351	5353	6488	2034	5540	4040	1148	
26.4	105.78	6890	3451	4894	5734	2357	5358	6494	2040	5529	4051	1160	
30.8	118.98	6892	3453	4899	5739	2360	5361	6502	2050	5519	4063	1174	
35.2	132.18	6895	3456	4902	5742	2369	5370	6513	2061	5518	4070	1188	
39.6	145.38	6902	3463	4907	5747	2380	5384	6522	2068	5505	4081	1205	
44.0	158.58	6916	3477	4916	5756	2392	5396	6530	2078	5498	4086	1227	
48.4	171.78	6928	3489	4924	5764	2402	5404	6538	2084	5491	4093	1256	
52.8	184.98	6935	3496	4934	5774	2412	5414	6546	2092	5482	4100	1316	
57.2	198.18	6947	3508	4946	5786	2426	5426	6596	2102	5472	4110	1416	
61.6	211.38	6961	3522	4962	5802	2434	5438	6562	2108	5463	4119	1511	

TABLE 10 (Cont.)

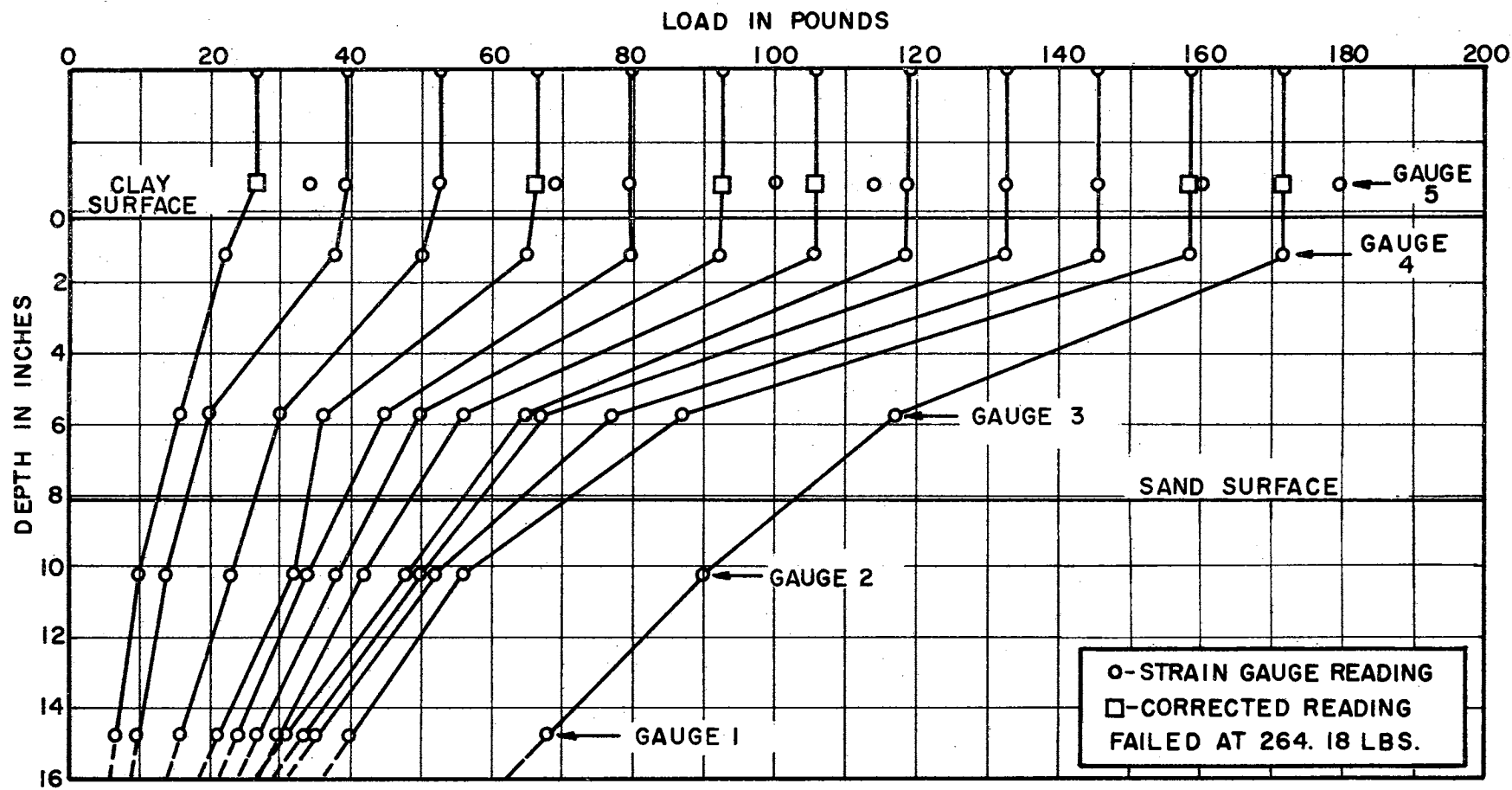| Load at Pan lbs	Load at Pile lbs	Gauge 1		Gauge 2		Gauge 3		Gauge 4				Dial Reading in x 10^{-4}	Time
		1S1	1S2	2S1	2S2	3S1	3S2	4S1	4S2	5S1	5S2		
66.0	224.58	6972	3533	4972	5812	2448	5448	6571	2117	5459	4123	1617	
70.4	237.78	6982	3543	4983	5823	2458	5458	6581	2127	5450	4132	1705	
74.8	250.98	6996	3557	4995	5835	2470	5476	6591	2137	5437	4145	1800	

FIGURE 25

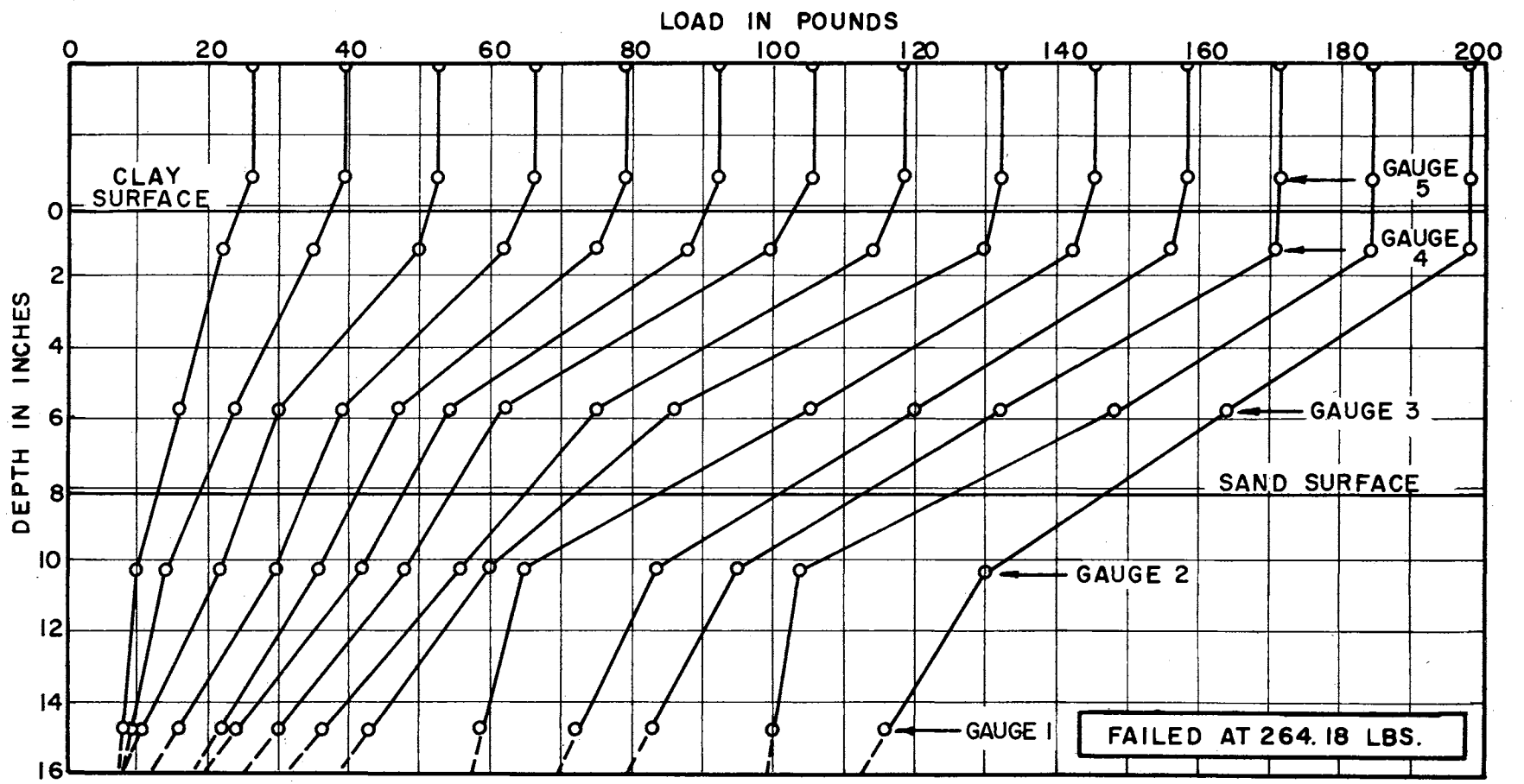LOAD DISTRIBUTION FOR PILE NO. 1 IN LAYERED SOIL

FIGURE 26

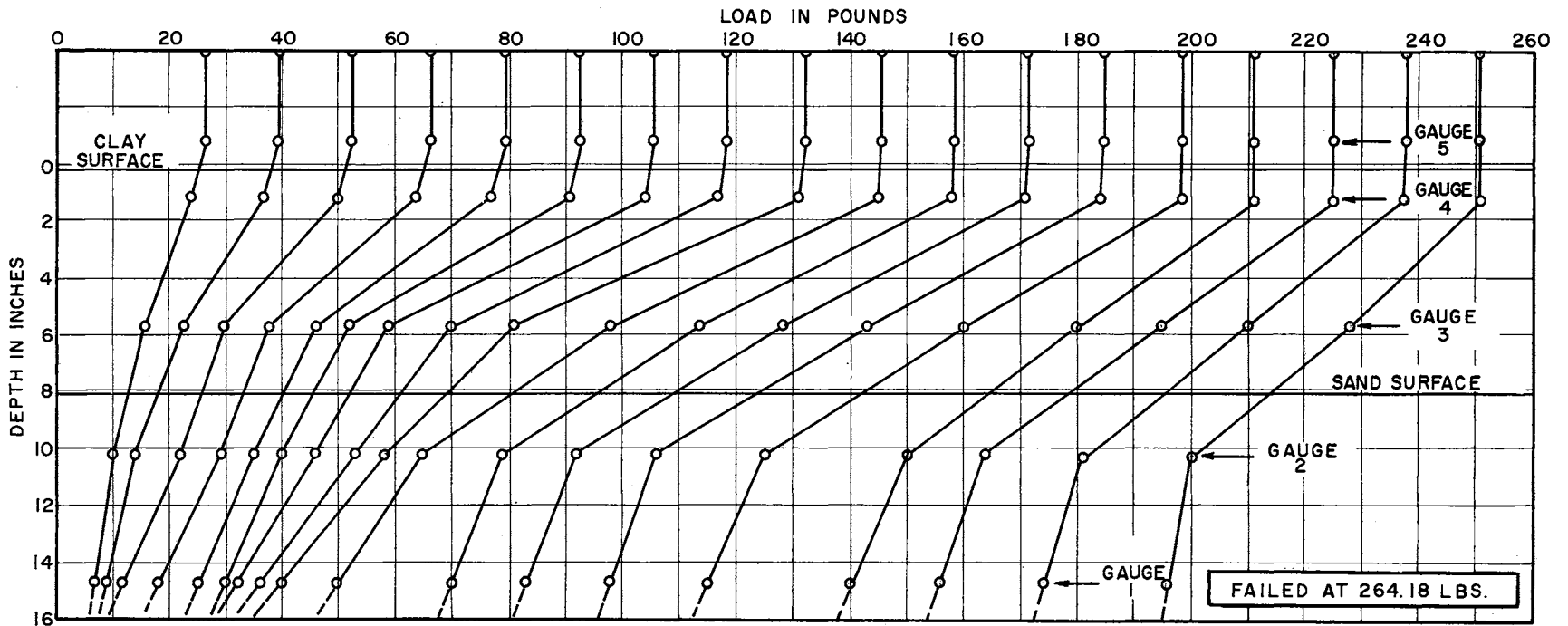LOAD DISTRIBUTION FOR PILE NO. 2 IN LAYERED SOIL

FIGURE 27

LOAD DISTRIBUTION FOR PILE NO. 3 IN LAYERED SOIL

the indicated values of the load increment. A comparison of the shapes of these curves with the ones pertaining to the load tests in sand and clay is interesting. There is good agreement among the curves in Figures 25, 26, and 27. There is a noticeable change in the shape of the curves where the applied load reached a magnitude of 160 to 180 pounds. This is believed to indicate a release of some of the load from the upper clay strata, and a consequent transfer of load to the lower sand strata, resulting in an appreciable increase in the load near the tip of pile. To avoid the effects of drift in the strain gauge readings, the load build up for pile 3 was not interrupted for the purpose of studying strains under sustained load. The incremental loadings were accomplished at a uniform rate until failure occurred, giving the results which are plotted in Figure 27. An examination of this figure indicates that when the load exceeds about fifty percent of the ultimate load the load transmitted to the pile tip is appreciable and increases rather uniformly until it reaches about seventy-five percent of the ultimate load. Thus the behavior of the model piles in the layered soil represents their behavior in clay soil up to about sixty-five percent of the applied load. For greater loads their behavior more nearly resembles that in sand.

The strain gauge readings at failure indicate that an appreciable amount of load is transferred to the soil along the whole length of the pile due to sliding friction. Monitoring of the soil surface during and after failure revealed no cracks or upheaval around the test pile, indicating that there was no shear failure in the clay layer and that the pile was supported by adhesion in this strata.

Figure 28 shows the relation between load and deflection for the three piles under incremental loading. An examination of these curves shows that the vertical deflection was in linear proportion to the applied load up to about seventy percent of the ultimate load, that there is very little vertical deflection up to about eighty-five percent of the ultimate load and that there is negligible increase of vertical deflection with time under sustained loading less than the ultimate load for each pile.

Finally the ultimate load under which the three piles failed was almost the same and was greater than that in clay or sand, indicating an improved ultimate load capacity in the layered soil as compared with the homogeneous soils.
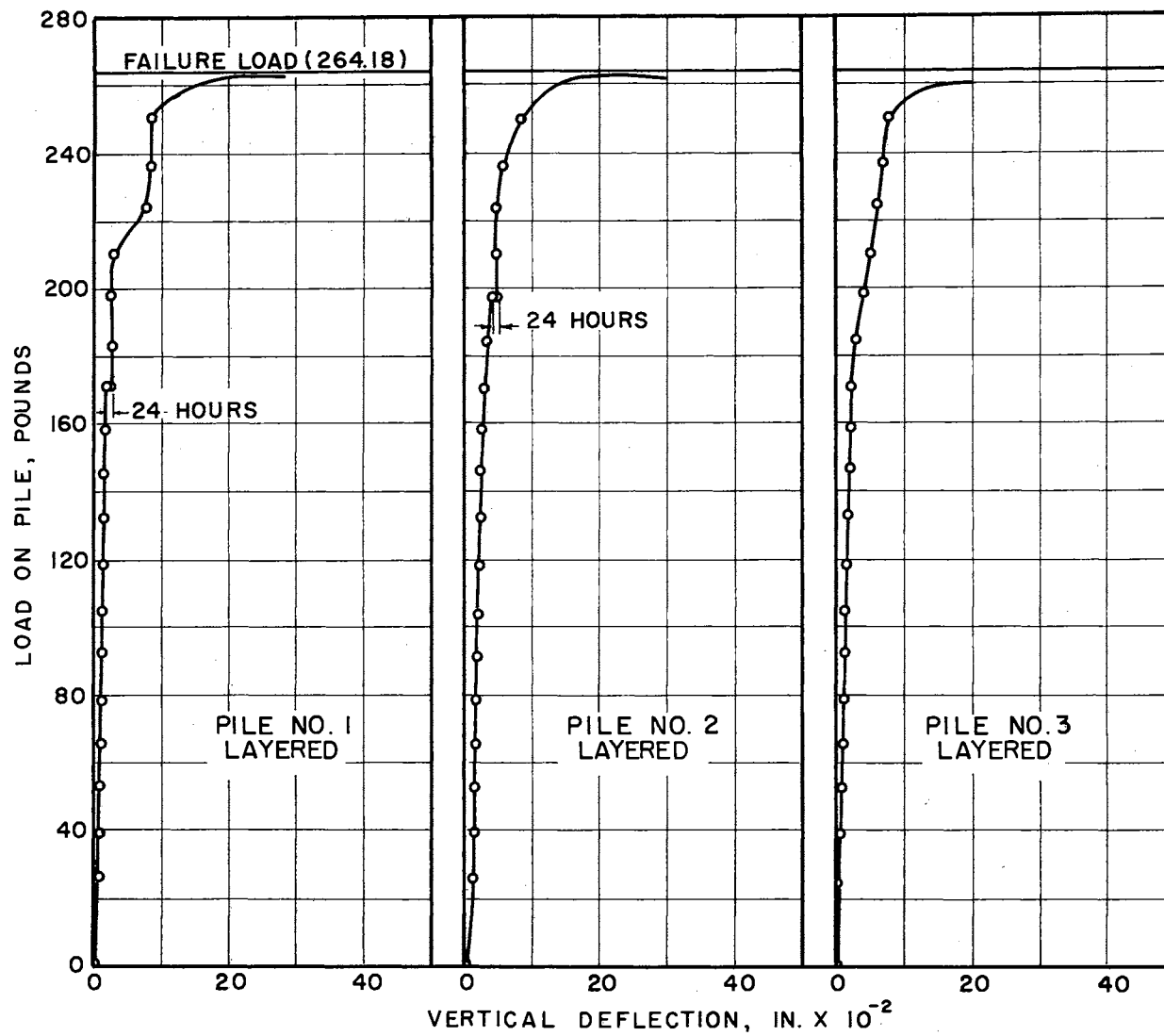
FIGURE 28

VERTICAL DEFLECTION UNDER LOAD IN LAYERED SOIL.

CHAPTER IV

CONCLUSIONS

The investigation program afforded an opportunity to measure and compare the stresses and loads along the length of model piles driven in different soils. It is felt that the results obtained provide information which was not readily available from load test data presented elsewhere.

Many interesting and valuable results were obtained, but it must be remembered that the investigation was conducted with only one type of pile, with only three different idealized soil conditions, and using a limited loading time. The possibility of different behavior under other conditions should not be overlooked. For example, the influences of type of pile, types of soil and soil systems, the geometry of the pile-soil system, and rate of load application still need to be investigated. However, the data obtained in this research appear to support the following conclusions in respect to model pile behavior under the restricted conditions employed in this study:

1. Almost all of the applied load is carried by point bearing for piles driven in sand. The smooth surface of the piles is believed to be the principal reason for the low frictional resistance observed.

2. For piles driven in clay soil the greatest part of the applied load is transferred to the adjacent soil by the adhesional resistance between the piles and the clay. The load transferred to the clay is mainly by the adhesion along the middle third of the embedded length of the pile,

with a tendency for the load to be transferred to lower parts of the pile with time. The maximum developed adhesion as determined from the slope of the load distribution curve of pile 3 was 1145 psf as compared to 4410 psf for the maximum shear stress of the clay soil.

3. The behavior of piles driven into a sand stratum underlying a clay stratum, with equal length of embedment in the two different strata, resembles that of a pile driven in clay up to about sixty-five percent of the total ultimate load on the pile. However, for applied loads greater than sixty-five percent of the total ultimate load the load distribution along the length of the driven pile approaches that of a pile driven into sand, with a greater percentage of load carried by point bearing.

4. There is a marked increase in the ultimate load for piles driven in the layered soil as compared to that for piles driven in homogenous soils (either sand or clay) for the same depth of embedment.

BIBLIOGRAPHY

1. Chellis, R. D., "Pile Foundations," 1961, McGraw-Hill.

2. Crandall, L. L., "Electrical Resistance Strain Gauges for Determining the Transfer of Load from Driven Piling to Soil," Proc. 2nd International Conference on Soil Mechanics and Foundation Engineering, 1948, Vol. 4, pp. 122-127.

3. VanWeele, Ir. A. F., "A Method of Separating the Bearing Capacity of a Test Pile into Skin Friction and Point-Resistance," Proc. 4th International Conference on Soil Mechanics and Foundation Engineering, 1957, Vol. II, pp. 76-80.

4. Seed, H. Bolton and Lymon C. Reese, "The Action of Soft Clay Along Friction Piles," Trans. ASCE, Paper No. 2882, Vol. 122, 1957, pp. 731-764.

5. Vey, Eben, "Frictional Resistance of Steel H-Piling in Clay," Proc., ASCE, Paper No. 1160, Vol. 83, January, 1957.

6. Mansur, Charles I. and Robert I. Kaufman, "Pile Tests, Low-Sill Structure, Old River, Louisiana," Trans., ASCE, Paper No. 2936, Vol. 123, 1958, pp. 715-748.

7. Mohane, D., G. S. Jain and V. Kumar, "Load Bearing Capacity of Piles," Geotech., Vol. 13, No. 1, March, 1963, p. 76.

8. D'Appolonia, E. and J. P. Romuldi, "Load Transfer in End Bearing Steel H-Piles," Journ. SM, ASCE, Vol. 89, No. SM 1 Proc. Paper 3450, March, 1963, pp. 1-25.

9. D'Appolonia, E. and J. A. Haribar, "Load Transfer in a Step Taper Pile," Jour. SM, ASCE, Vol. 89, No. SM 6, Proc. Paper 3700, November, 1963.

10. Mueller, R., "Model Study of the Interrelation of Friction, Point Resistance, and Bearing Capacity of Piles," (in German) DEGEBO, Berlin, 1939.

11. Khalifa, Mohamed K., "Model Studies of Pile Foundations," Bulletin No. 7, Civil Engineering Research Laboratory, Columbia University, 1940.

12. Davis, E. I. and H. E. Webster, "Abstracts of Selected Theses on Soil Mechanics, Part III: Investigation by Model of Skin Friction and Point Resistance of Piles," MIT, 1941.

66

13. Krome, John E., "Preliminary Study of the Application of Electric Resistivity Strain Gauges to Tests on Model Piles," Unpublished student paper, Princeton University, 1941.

14. Florentin, J. G. L'Heriteau, and M. Farhi, "Tests on Small Sized Model Piles," Proc. 2nd International Conference on Soil Mechanics and Foundation Engineering, 1948, Vol. 5, pp. 154-155.

15. Ghanem, M. F., "Bearing Capacity of Friction Piles in Deep Soft Clays," Thesis presented to the University of Illinois, Urbana, Illinois, 1953, in partial fulfillment of the requirements for the degree of Doctor of Philosophy.

16. Gamal El Din, A. K., "The Bearing Capacity of Piles in Relation to the Properties of Clay," Proc. of the 5th International Conference on Soil Mechanics and Foundation Engineering, 1961, Vol. 2, pp. 59-63.

17. Bowman, J. W., "The Effects of Gypsum on the Strength of Clay," Thesis presented to Oklahoma State University, Stillwater, Oklahoma, 1963, in partial fulfillment of the requirements for the degree of Master of Science.

VITA

Laith Ismail Namiq

Candidate for the Degree of

Master of Science

Thesis: STRESS VARIATION ALONG THE LENGTH OF MODEL PILES

Major Field: Civil Engineering

Biographical:

Personal Data: Born in Baghdad, Iraq, July 5, 1939, the son of Ismail and Karima Namiq.

Education: Graduated from Baghdad College High School, Baghdad, Iraq, June, 1955; received the degree of Bachelor of Science, with a major in Civil Engineering, from the University of Baghdad in June, 1959; completed the requirements for Master of Science in May, 1965.

Professional Experience: Design Engineer in the Design Center, Ministry of Works and Housing, Iraq, from July, 1959 to September, 1959; Second Lieutenant, Directorate of Millitary Works, Iraqi Army from February, 1960 to November, 1962; Staff Engineer in the Directorate General of Industrial Buildings, Ministry of Industry from November, 1962 to July, 1963; Assistant Scientific Researcher, University of Baghdad from July, 1963, to September, 1964; Part-time Engineer, the Soil Mechanics Laboratory, Consulting Foundations Engineers, Baghdad, Iraq, from July, 1959, to September, 1964. Acting as the Director from November, 1963, to September, 1964.

Professional Societies: Associate Member of the American Society of Civil Engineers, Junior Member American Concrete Institute, Member and Editorial Secretary of Al Muhandis, the Journal of the Iraqi Society of Engineers.

Honorary Societies: Member of Chi Epsilon; Associate Member of the Society of the Sigma Xi.